SPATIAL SEGREGATION IN REACTION-DIFFUSION EPIDEMIC MODELS

HAO WANG[†], KAI WANG[‡], AND YONG-JUNG KIM[§]

Abstract. In this paper, we formulate SIS reaction-diffusion epidemic models with cognition and show the impact of movement strategies on disease outbreak and mitigation under a spatially heterogeneous environment. The cognitive diffusion either takes a Fokker-Planck type diffusion obtained by Chapman's diffusion law (called random diffusion) or follows Fick's diffusion law (called symmetric diffusion). We derive a variational expression of the basic reproduction number $\mathcal{R}_0$ for both models and prove that the disease-free equilibrium is unique and globally asymptotically stable if $\mathcal{R}_0 < 1$. Furthermore, if $\mathcal{R}_0 > 1$, the model following Fick's diffusion law admits at least one endemic equilibrium and the model following Chapman's diffusion law has a unique endemic equilibrium. The theoretical results are illustrated by numerical simulations, which additionally show the segregation phenomenon between susceptible and infected populations regulated by different movement strategies. Spatial segregation here is natural, not caused by an isolation policy, and thus is the most important indicator for an infectious disease to spread or wane in the absence of intervention. The first example shows that a heterogeneous random diffusion segregates infected and susceptible populations further than an ODE model and thus reduces the infection size. However, symmetric diffusion never does that. The second example shows that a heterogeneous random diffusion detriments segregation but still reduces the infection severity by moving infected individuals to a disease-free region. In a certain situation, a heterogeneous random diffusion may increase the infection severity as shown in the last example.

Keywords: spatial heterogeneity, cognitive movement, basic reproduction number, disease-free equilibrium, endemic equilibrium, segregation

2020 Mathematics Subject Classification. 35K57, 92D30, 91D25, 37N25

1. Introduction

Mathematical models are powerful tools to study disease transmission and control. The most widely used models are ordinary differential equation (ODE) compartment models that determine whether an infectious disease will surge or not by the basic reproduction number $\mathcal{R}_0$ compared with one. Population movement and spatial heterogeneity are obviously significant in disease spread and mitigation. Toward this aspect, various partial differential equation (PDE) and network models have been proposed in the literature (see [1, 7, 23, 30, 31]).

To study the effect of spatial heterogeneity and diffusive population on the disease dynamics, Allen *et al.* [1] developed an SIS (susceptible-infected-susceptible) reaction-diffusion epidemic model:

$$\begin{aligned} &S_t = d_S\Delta S - \Big(\tfrac{\beta(x)S}{S+I} - r(x)\Big)I, && t>0,\ x\in\Omega,\\ &I_t = d_I\Delta I + \Big(\tfrac{\beta(x)S}{S+I} - r(x)\Big)I, && t>0,\ x\in\Omega,\\ &\nabla S\cdot\mathbf{n} = \nabla I\cdot\mathbf{n} = 0, && t>0,\ x\in\partial\Omega,\\ &S(x,0)=S_0(x),\ I(x,0)=I_0(x), && t=0,\ x\in\Omega, \end{aligned} \tag{1.1}$$

where $\Omega\in\mathbb{R}^m$ ($m\geq 1$) is a bounded domain with smooth boundary $\partial\Omega$ ($m>1$) and $\mathbf{n}$ is the outward unit normal vector on $\partial\Omega$. The variables $S(t,x)$ and $I(t,x)$ represent the population densities of susceptible and infected individuals, respectively, at time $t>0$ and location $x\in\Omega$. The diffusion rates d_S and d_I are positive constants. The spatial functions $\beta(x)$ and $r(x)$ represent disease transmission rate and recovery rate at x, and they are Hölder continuous functions on $\overline{\Omega}$.

[†]Corresponding author. Department of Mathematical and Statistical Sciences, University of Alberta, Edmonton, AB T6G 2G1, Canada (hao8@ualberta.ca).

[‡]Department of Mathematics, Nanjing University of Aeronautics and Astronautics, Nanjing 211106, China, and Key Laboratory of Mathematical Modelling and High Performance Computing of Air Vehicles (NUAA), MIIT, Nanjing 211106, China, and Department of Mathematical and Statistical Sciences, University of Alberta, Edmonton, AB T6G 2G1, Canada (kwang@nuaa.edu.cn, kai9@ualberta.ca).

[§]Department of Mathematical Sciences, KAIST, 291 Daehak-ro, Yuseong-gu, Daejeon 305-701, Korea (yongkim@kaist.edu).

Allen *et al.* derived a variational expression of the basic reproduction number for the PDE system (1.1) as follows:

$$\mathcal{R}_0 = \sup_{\phi\in W^{1,2}(\Omega),\phi\neq 0}\left\{\frac{\int_\Omega \beta\phi^2 \mathrm{d}x}{\int_\Omega d_I|\nabla\phi|^2\mathrm{d}x+\int_\Omega r\phi^2\mathrm{d}x}\right\}.$$

Moreover, they showed the monotone and asymptotic behavior of $\mathcal{R}_0$ on the diffusion rate d_I. In particular, the existence and stability of the disease-free equilibrium and the asymptotic behavior of an endemic equilibrium were investigated mathematically. One can find many follow-up papers [3–5, 14, 15, 21, 22, 32]. However, all these studies assumed the simplest diffusion terms with constant diffusion rates.

Although the spatial heterogeneity of the model (1.1) was considered in the transmissibility $\beta(x)$ and the recovery $r(x)$, the simplest diffusion terms were assumed mimicking particle movement. However, humans have cognition that is crucial in the mechanistic modeling of any organisms with perception, memory and learning. To model the cognitive movement, we start with dispersal on a patch system. Let u_i be the population in patch i. Denote c_{ij} $(c_{i\leftarrow j})$ as the migration or departing rate from patch j to patch i (see Fig. 1). Then, the rate of change of population u_i satisfies

$$\dot{u}_i = c_{ii-1}u_{i-1} + c_{ii+1}u_{i+1} - c_{i-1i}u_i - c_{i+1i}u_i. \tag{1.2}$$

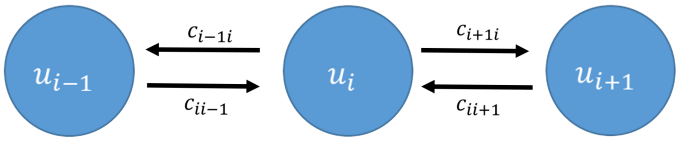

FIGURE 1. Scheme of dispersal between patches.

If $c_{ii+1} = c_{i+1i}$, i.e., the dispersal rate of population from patch i to $i+1$ is equal to that from patch $i+1$ to i, the dispersal is called *symmetric* (see [12]). If we denote $\gamma_{i+1/2} := c_{ii+1} = c_{i+1i}$, (1.2) is rewritten as

$$\dot{u}_i = \gamma_{i+1/2}(u_{i+1}-u_i) - \gamma_{i-1/2}(u_i-u_{i-1}) \cong \gamma_{i+1/2}u'_{i+1/2} - \gamma_{i-1/2}u'_{i-1/2} \cong (\gamma u')'_i.$$

In this approximation, the distance between two adjacent patches is one, which is treated as sufficiently small. In a space with any dimension, this relation is written as a PDE:

$$u_t = \nabla\cdot(\gamma(x)\nabla u), \tag{1.3}$$

which follows Fick's diffusion law. The physical meaning of this symmetric diffusion is unclear. We are more interested in the case when $c_{i-1i} = c_{i+1i}$, i.e., when the dispersal rate from patch i to $i-1$ is equal to the one from patch i to $i+1$. In this case, the probabilities of moving to the right patch or to the left patch are identical and hence, the dispersal is called *random*. If we denote $\gamma_i := c_{i+1i} = c_{i-1i}$, (1.2) is written as

$$\dot{u}_i = \gamma_{i-1}u_{i-1} + \gamma_{i+1}u_{i+1} - 2\gamma_i u_i \cong (\gamma u)''_i.$$

The corresponding PDE model in any spatial dimension is

$$u_t = \Delta(\gamma(x)u), \tag{1.4}$$

which follows Chapman's diffusion law. The physical meaning of this random diffusion is clear. Such a random diffusion is also called Fokker-Planck type or Ito type. If the dispersal is random and symmetric at the same time, all of c_{ij} coefficients are equal, which leads to the spatially homogeneous diffusion. For more model formulations on diffusion, readers can refer to [19, 24] and references therein.

By considering spatially heterogeneous movements, we propose the following SIS reaction-diffusion epidemic model with random diffusion (or Fokker-Planck type):

$$\begin{aligned}
&S_t = \Delta(f(x)S) - \left(\tfrac{\beta(x)S}{S+I} - r(x)\right)I, && t>0,\ x\in\Omega,\\
&I_t = \Delta(g(x)I) + \left(\tfrac{\beta(x)S}{S+I} - r(x)\right)I, && t>0,\ x\in\Omega,\\
&\nabla(f(x)S)\cdot\mathbf{n} = \nabla(g(x)I)\cdot\mathbf{n} = 0, && t>0,\ x\in\partial\Omega,\\
&S(0,x)\geq,\not\equiv 0,\ I(0,x)\geq,\not\equiv 0, && x\in\overline{\Omega},
\end{aligned} \tag{1.5}$$

where $f(x)$ and $g(x)$ are dispersal rates of susceptible and infected groups at x, respectively. For comparison, we investigate the properties of a corresponding model with symmetric diffusion (or Fickian type):

$$\begin{aligned}
&S_t = \nabla\cdot(f(x)\nabla S) - \left(\tfrac{\beta(x)S}{S+I} - r(x)\right)I, && t>0,\ x\in\Omega,\\
&I_t = \nabla\cdot(g(x)\nabla I) + \left(\tfrac{\beta(x)S}{S+I} - r(x)\right)I, && t>0,\ x\in\Omega,\\
&\nabla S\cdot\mathbf{n} = \nabla I\cdot\mathbf{n} = 0, && t>0,\ x\in\partial\Omega,\\
&S(0,x)\geq,\not\equiv 0,\ I(0,x)\geq,\not\equiv 0, && x\in\overline{\Omega}.
\end{aligned} \tag{1.6}$$

However, the symmetric diffusion shows similar dynamical behaviors as a homogeneous diffusion (see Section 5). Note that the Fokker-Planck type diffusion is written as

$$\Delta(f(x)S) = \nabla\cdot(f(x)\nabla S) + \nabla\cdot(S\nabla f(x)).$$

Hence, the advection term $\nabla\cdot(S\nabla f(x))$ is the difference between the two diffusion laws.

It is natural to expect that susceptible and infected individuals disperse differently. We assume that the dispersal rate f of the susceptible population S is an increasing function of the transmission rate β since the infection probability is the primary concern of healthy people. In other words, when susceptible people are located in a region with a high transmission rate $\beta(x)$ (such as indoor playground), they will leave to avoid infection. On the other hand, we assume that the dispersal rate g of the infected population I is an increasing function of the reciprocal of the recovery rate r^{-1}. In fact, infected people only care about recovery (or treatment). For example, if infected people are located in a region with a high recovery rate $r(x)$ (such as hospital), they will prefer to stay there for faster recovery. As a summary, these two groups of people have their own dispersal strategies based on their cognition (see [2, 10, 11]). This model formulation is an application of our cognitive movement modeling efforts [28] in epidemiological modeling.

In the proposed models, we have four functions f, g, β and r. We assume these functions and initial values satisfy following hypotheses:

(H1) There exist constants m_0 and M_0 such that

$$0 < m_0 < f, g < M_0 < \infty,$$

which is used for the uniform parabolicity of the problem.

(H2) f and g are increasing functions of β and r^{-1}, respectively, i.e.,

$$f = f(\beta) \text{ and } g = g(r^{-1})$$

are monotone increasing.

(H3) The set $\Omega^+ := \{x \in \Omega : \beta(x) > r(x)\}$ is nonempty.

Most studies on infectious disease PDE models mainly focused on asymptotic behaviors for sufficiently large time. However, few studies have been done on the transient dynamics of epidemiological models due to lack of appropriate mathematical tools. In this paper, we study the transient dynamics of systems (1.5), (1.6) and (1.1) through numerical simulations. We will explore the spatial segregation induced by cognitive diffusion, the use of disease-free region, and negative effects of mixing by diffusion. Biological segregation is a phenomenon that population groups are separated in certain areas [26]. To measure the degree of segregation, we define the segregation indices

$$\kappa(v_1, v_2) = \frac{\|v_1 - v_2\|_{L^1(\Omega)}}{\|v_1\|_{L^1(\Omega)} + \|v_2\|_{L^1(\Omega)}} \tag{1.7}$$

and

$$\chi(v_1, v_2) = \max_{x\in\Omega}\{v_1(x) - v_2(x)\}\cdot\min_{x\in\Omega}\{v_1(x) - v_2(x)\} \tag{1.8}$$

for $v_i(x) \in L^1(\Omega)$ and $\|v_i\|_{L^1(\Omega)} = \int_\Omega |v_i(x)|\mathrm{d}x$, $i = 1, 2$. Obviously $0 \le \kappa(v_1, v_2) \le 1$. If $\kappa(v_1, v_2)$ is large and $\chi(v_1, v_2) \le 0$, then the segregation phenomenon between v_1 and v_2 is more obvious (so called perfect/strong segregation). If $\kappa(v_1, v_2)$ is small and $\chi(v_1, v_2) \le 0$, then the segregation phenomenon is less obvious (so called weak segregation). If $\kappa(v_1, v_2) = 0$ or $\chi(v_1, v_2) > 0$, then the segregation phenomenon disappears.

The main goals of the paper are as follows: (i) The variational characterizations of the basic reproduction number $\mathcal{R}_0$ for systems (1.5) and (1.6) are defined, respectively, and then the monotonic and asymptotic behaviors of $\mathcal{R}_0$ on the diffusion rate g are discussed; (ii) We prove the existence and stability of disease-free equilibrium (DFE) and endemic equilibrium (EE) of (1.5) and (1.6) respectively, and verify the theoretical results by numerical simulations; More importantly, (iii) we investigate the segregation phenomena of (1.5), (1.6) and (1.1) numerically. It is worth mentioning that there are several significant improvements. Firstly, in modeling we propose two new models with different diffusion mechanisms and assume that the dispersal rates of susceptible and infected individuals depend on the transmission and recovery rates, respectively. Secondly, in terms of theory we generalize the results of [1, Lemmas 2.2-2.3] on the monotonicity of $\mathcal{R}_0$ for model (1.6) (see Lemmas 2.1-2.2, 3.2-3.3). Finally, spatial segregation occurs naturally here (not caused by an isolation policy) and thus is the most important indicator for an infectious disease to spread or wane in the absence of intervention.

The remaining paper is organized as follows. In sections 2 and 3, we show the existence and stability of DFE and EE for the models (1.6) and (1.5). In section 4, our theoretical results are verified by numerical simulations. In section 5, we consider three numerical examples to illustrate the segregation phenomena of epidemic PDE models and their impact on the disease spread. Section 6 summarizes this paper with a brief discussion.

2. The epidemic model with symmetric diffusion

In this section, we prove the existence and stability of DFE and EE for model (1.6) with symmetric diffusion. We start with the well-posedness result.

Proposition 2.1. *The system (1.6) admits a unique positive solution $S(t,x)$ and $I(t,x)$ satisfying*

$$(S(t,x), I(t,x)) \in C^{2,1}((0,\infty)\times\overline{\Omega}) \times C^{2,1}((0,\infty)\times\overline{\Omega}).$$

Furthermore, there is a constant $C>0$ independent of the initial values, and $T_0>0$ such that the solution $(S(t,x), I(t,x))$ meets

$$\|S(t,x)\|_{L^\infty(\Omega)} + \|I(t,x)\|_{L^\infty(\Omega)} \le C, \quad \text{for all} \quad t > T_0.$$

Proof. (i) According to the regularity theory of parabolic equations [20], the system (1.6) possesses a unique nonnegative classical solution $(S(t,x), I(t,x)) \in C^{2,1}((0,\infty)\times\overline{\Omega}) \times C^{2,1}((0,\infty)\times\overline{\Omega})$. Moreover, applying strong maximum principle [25] yields that $S(t,x)$ and $I(t,x)$ are positive, for any $x\in\overline{\Omega}$ and $t>0$.

(ii) Adding two equations of (1.6) and then integrating over Ω, we get

$$\int_\Omega ((S(t,x)+I(t,x)))_t \mathrm{d}x = (f(\beta(x))\nabla S + g(r^{-1}(x))\nabla I)|_{\partial\Omega} = 0.$$

which is owing to $\nabla S\cdot\mathbf{n} = \nabla I\cdot\mathbf{n} = 0$ on $\partial\Omega$. Thus, we obtain

$$\int_\Omega ((S(t,x)+I(t,x)))\mathrm{d}x = N_0, \tag{2.1}$$

for some constant $N_0>0$. In particular, $N_0 = \int_\Omega (S_0(x)+I_0(x))\mathrm{d}x$. This means that the $L^1(\Omega)$ norms of $S(t,\cdot)$ and $I(t,\cdot)$ are bounded. Hence, by [6] ($p_0=1$, $\sigma=1$) and the positivity of $S(t,\cdot)$ and $I(t,\cdot)$, there exists a constant $C>0$, independent of $S_0(\cdot)$ and $I_0(\cdot)$, and $T_0>0$ such that

$$\|S(t,x)\|_{L^\infty(\Omega)} + \|I(t,x)\|_{L^\infty(\Omega)} \le C,$$

for all $t>T_0$. The proof is completed. □

2.1. The disease-free equilibrium.

In this subsection, we derive the basic reproduction number of model (1.6) and discuss the stability of DFE of (1.6).

By direct calculations, the model (1.6) has a unique DFE $E_0 = (\tilde{S}_0, 0) := (N_0/|\Omega|, 0)$. Linearizing system (1.6) at E_0 gives

$$\begin{aligned} &\overline{S}_t = \nabla\cdot(f(\beta(x))\nabla\overline{S}) - (\beta(x)-r(x))\overline{I}, && t>0,\ x\in\Omega,\\ &\overline{I}_t = \nabla\cdot(g(r^{-1}(x))\nabla\overline{I}) + (\beta(x)-r(x))\overline{I}, && t>0,\ x\in\Omega,\\ &\nabla\overline{S}\cdot\mathbf{n} = \nabla\overline{I}\cdot\mathbf{n} = 0, && t>0,\ x\in\partial\Omega, \end{aligned} \tag{2.2}$$

where

$$\overline{S}(t,x) = S(t,x) - \tilde{S}_0 \ \text{ and } \ \overline{I}(t,x) = I(t,x). \tag{2.3}$$

Since $\overline{S}$ is decoupled, it suffices to consider the following system:

$$\begin{aligned} &\overline{I}_t = \nabla\cdot(g(r^{-1}(x))\nabla\overline{I}) + (\beta(x)-r(x))\overline{I}, && t>0,\ x\in\Omega,\\ &\nabla\overline{I}\cdot\mathbf{n} = 0, && t>0,\ x\in\partial\Omega. \end{aligned} \tag{2.4}$$

Letting $\overline{I}(t,x) = e^{-\zeta t}\phi(x)$ and substituting it into (2.4) results in

$$\begin{aligned} &\nabla\cdot(g(r^{-1}(x))\nabla\phi) + (\beta(x)-r(x))\phi + \zeta\phi = 0, && x\in\Omega,\\ &\nabla\phi\cdot\mathbf{n} = 0, && x\in\partial\Omega. \end{aligned} \tag{2.5}$$

Similar to the analysis of [1, (2.2)], the eigenvalue problem (2.5) has at least one eigenvalue ζ^* corresponding to the positive eigenfunction ϕ^*, while other eigenvalues do not have a positive eigenfunction. Then (ζ^*,ϕ^*) satisfies

$$\begin{aligned} &\nabla\cdot(g(r^{-1}(x))\nabla\phi^*) + (\beta(x)-r(x))\phi^* + \zeta^*\phi^* = 0, && x\in\Omega,\\ &\nabla\phi^*\cdot\mathbf{n} = 0, && x\in\partial\Omega. \end{aligned} \tag{2.6}$$

Moreover, ζ^* is expressed by the following variational characterization:

$$\zeta^* = \inf_{\phi\in W^{1,2}(\Omega),\phi\neq 0}\left\{\frac{\int_\Omega g((r^{-1}))|\nabla\phi|^2\mathrm{d}x + \int_\Omega (r-\beta)\phi^2\mathrm{d}x}{\int_\Omega \phi^2\mathrm{d}x}\right\}, \tag{2.7}$$

where ζ^* and ϕ^* are differentiable with respect to $g(\cdot)$.

Lemma 2.1. *Define ζ^* by (2.7) and assume $g(r^{-1}(\cdot)) = \eta g_1(r^{-1}(\cdot))$, where η and g_1 are a positive constant and $C^3(\overline{\Omega})$ function, respectively. Then the following properties hold:*
(i) *If $\beta(x) - r(x)$ changes sign on Ω, and*

$$\overline{g}(x)(\phi^*)^2(x) \le 0 \text{ on } \partial\Omega, \text{ and } \overline{g}'(x) \ge 0 \text{ on } \Omega,$$

then ζ^* is a strictly monotone increasing function with respect to g;
(ii) *$\zeta^* \to \min_{x\in\overline{\Omega}}\{r(x) - \beta(x)\} < 0$, as $\eta \to 0$, for fixed g_1;*
(iii) *$\zeta^* \to \frac{1}{|\Omega|}\int_\Omega (r(x) - \beta(x))\mathrm{d}x$, as $\eta \to \infty$, for fixed g_1;*
(iv) *If $\int_\Omega r(x)\mathrm{d}x \le \int_\Omega \beta(x)\mathrm{d}x$, then $\zeta^* < 0$ for any $g > 0$;*
(v) *If $\int_\Omega r(x)\mathrm{d}x > \int_\Omega \beta(x)\mathrm{d}x$, then for fixed g_1, $\zeta^*(\eta) = 0$ admits a unique root $\eta^* > 0$ such that $\zeta^* < 0$ when $\eta < \eta^*$, and $\zeta^* > 0$ when $\eta > \eta^*$.*

Proof. (i) By (2.7), it is obvious that ζ^* is an increasing function of g. Next, it is only necessary to prove that the monotonicity is strict. Differentiating the first equation of system (2.6) with respect to g, we obtain

$$\begin{aligned} &\Delta\phi^* + g\Delta\phi_g^* + \bar{g}\nabla\phi^* + g'\nabla\phi_g^* + (\beta(x) - r(x))\phi_g^* + \zeta_g^*\phi^* + \zeta^*\phi_g^* = 0, && x \in \Omega,\\ &\nabla\phi^* \cdot \mathbf{n} = \nabla\phi_g^* \cdot \mathbf{n} = 0, && x \in \partial\Omega, \end{aligned} \tag{2.8}$$

where $\bar{g} = g''/g'$, $\phi_g^* = \mathrm{d}\phi^*/\mathrm{d}g$ and the prime represents the derivative with respect to the spatial variable x. Multiplying the first equations of (2.8) and (2.6) by ϕ^* and ϕ_g^* respectively and then integrating by parts over Ω leads to

$$\begin{aligned} &-\int_\Omega |\nabla\phi^*|^2\mathrm{d}x - \int_\Omega g'\phi^*\nabla\phi_g^*\mathrm{d}x - \int_\Omega g\nabla\phi^*\nabla\phi_g^*\mathrm{d}x + \frac{1}{2}(\overline{g}(\phi^*)^2)|_{\partial\Omega} - \frac{1}{2}\int_\Omega \overline{g}'(\phi^*)^2\mathrm{d}x\\ &+\int_\Omega g'\phi^*\nabla\phi_g^*\mathrm{d}x + \int_\Omega (\beta(x) - r(x))\phi^*\phi_g^*\mathrm{d}x + \zeta_g^*\int_\Omega (\phi^*)^2\mathrm{d}x + \zeta^*\int_\Omega \phi^*\phi_g^*\mathrm{d}x = 0 \end{aligned}$$

and

$$\begin{aligned} &-\int_\Omega g'\phi_g^*\nabla\phi^*\mathrm{d}x - \int_\Omega g\nabla\phi_g^*\nabla\phi^*\mathrm{d}x + \int_\Omega g'\phi_g^*\nabla\phi^*\mathrm{d}x + \int_\Omega (\beta(x) - r(x))\phi_g^*\phi^*\mathrm{d}x\\ &+\zeta^*\int_\Omega \phi^*\phi_g^*\mathrm{d}x = 0. \end{aligned}$$

Subtracting the above two equations leads to

$$\zeta_g^*\int_\Omega (\phi^*)^2\mathrm{d}x = \int_\Omega |\nabla\phi^*|^2\mathrm{d}x - \frac{1}{2}(\overline{g}(\phi^*)^2)|_{\partial\Omega} + \frac{1}{2}\int_\Omega \overline{g}'(\phi^*)^2\mathrm{d}x. \tag{2.9}$$

Case 1. If

$$\overline{g}(x)(\phi^*)^2(x) \le 0 \text{ on } \partial\Omega \quad \text{and} \quad \overline{g}'(x) > 0 \text{ on } \Omega$$

or

$$\overline{g}(x)(\phi^*)^2(x) < 0 \text{ on } \partial\Omega \quad \text{and} \quad \overline{g}'(x) \ge 0 \text{ on } \Omega,$$

then $\zeta_g^* > 0$ since ϕ^* is a positive function on Ω.
Case 2. If

$$\overline{g}(x) \equiv 0 \text{ on } \partial\Omega \quad \text{and} \quad \overline{g}'(x) \equiv 0 \text{ on } \Omega,$$

then $\overline{g} \equiv 0$ in Ω. Thus, $g''(x) \equiv 0$ on Ω. Furthermore, we have $g(x) = C_1x + C_2$ for some constants C_1 and C_2, $x \in \Omega$. In this case, the formula (2.9) is rewritten as

$$\zeta_g^*\int_\Omega (\phi^*)^2\mathrm{d}x = \int_\Omega |\nabla\phi^*|^2\mathrm{d}x,$$

which indicates that $\zeta_g^* \ge 0$ for any ϕ^* and $\zeta_g^* = 0$ if and only if ϕ^* is a positive constant. Assuming ϕ^* is a positive constant, it follows from (2.6) that

$$(\beta(x) - r(x)) + \zeta^* = 0, \ \ x \in \Omega.$$

This is a contradiction with the fact that $\beta(x) - r(x)$ changes sign in Ω. Therefore, $\zeta_g^* > 0$.
(ii) The conclusion is the direct result of [17, Lemma 3.1].
(iii) In (2.7), we choose $\phi = 1/|\Omega|$. Then

$$\zeta^* = \frac{1}{|\Omega|}\int_\Omega (r(x) - \beta(x))\mathrm{d}x \le \max_{x\in\Omega}\{r(x) - \beta(x)\}.$$

According to the definition of ζ^*, one has

$$\zeta^* \le \max_{x\in\Omega}\{r(x) - \beta(x)\}, \text{ for any } \phi(\cdot) \in W^{1,2}(\Omega) \text{ and } \eta > 0.$$

Thus, by (i) and utilizing the monotone bounded convergence theorem, there exists a constant $\zeta_\infty^* < \infty$ such that $\zeta^* \to \zeta_\infty^*$ when η tends to ∞. Dividing both sides of equation (2.6) by η yields

$$\nabla \cdot (g_1(r^{-1})\nabla\phi^*) + \frac{\beta(x) - r(x) + \zeta^*}{\eta} = 0.$$

According to the elliptic regularity, there is a positive constant ϕ_∞^* such that ϕ^* converges to ϕ_∞^* in $C(\overline{\Omega})$ as $\eta \to \infty$. Consequently, integrating (2.6) over Ω, we have

$$\int_\Omega (\beta(x) - r(x))\phi^* \mathrm{d}x + \zeta^* \int_\Omega \phi^* \mathrm{d}x = 0$$

which implies that $\zeta^* \to \frac{1}{|\Omega|}\int_\Omega (r(x) - \beta(x))\mathrm{d}x$ as $\eta \to \infty$.

(iv) From (ii), as $g \to \infty$, we have

$$\zeta^* \to \frac{1}{|\Omega|}\int_\Omega (r(x) - \beta(x))\mathrm{d}x \le 0.$$

Hence, $\zeta^* < 0$ for any $g > 0$ since ζ^* is a strictly increasing function of g. Moreover, by inspiration of (i)-(iv), the proof of (v) is obvious and so we omit it. □

Remark 2.1. *The conditions in (i) of Lemma 2.1 include the case that the diffusion coefficient is constant [1]. In fact, when $g(r^{-1}) \equiv$ constant, then*

$$\overline{g}(x) \equiv 0 \ \text{ on } \partial\Omega, \ \text{ and } \ \overline{g}'(x) \equiv 0 \ \text{ on } \Omega.$$

Equivalently, ***Case 2*** *holds.*

In order to explore the stability of DFE, it is necessary to derive the basic reproduction number $\mathcal{R}_0$ of system (1.6). To this end, we analyze the following eigenvalue problem:

$$\begin{aligned} &\nabla \cdot (g(r^{-1}(x))\nabla\phi) - r(x)\phi + \zeta\beta(x)\phi = 0, && x \in \Omega, \\ &\nabla\phi \cdot \mathbf{n} = 0, && x \in \partial\Omega, \end{aligned} \tag{2.10}$$

and obtain the following results.

Lemma 2.2. *Let ζ_0 be a positive eigenvalue of (2.10) with a positive eigenfunction and assume $g(r^{-1}(\cdot)) = \eta g_1(r^{-1}(\cdot))$. Then ζ_0 is unique and*

$$\zeta_0 = \inf_{\phi \in W^{1,2}(\Omega), \phi \neq 0} \left\{ \frac{\int_\Omega g((r^{-1}))|\nabla\phi|^2 \mathrm{d}x + \int_\Omega r\phi^2 \mathrm{d}x}{\int_\Omega \beta\phi^2 \mathrm{d}x} \right\}. \tag{2.11}$$

Furthermore, the basic reproduction number $\mathcal{R}_0$ of (1.6) is defined by

$$\mathcal{R}_0 = \sup_{\phi \in W^{1,2}(\Omega), \phi \neq 0} \left\{ \frac{\int_\Omega \beta\phi^2 \mathrm{d}x}{\int_\Omega g((r^{-1}))|\nabla\phi|^2 \mathrm{d}x + \int_\Omega r\phi^2 \mathrm{d}x} \right\}. \tag{2.12}$$

Moreover, if $\beta(x) - r(x)$ changes sign on Ω, then $\mathcal{R}_0$ satisfies the following properties:
(i) *$\mathcal{R}_0 = 1/\zeta_0$ is monotone decreasing with respect to g;*
(ii) *$\mathcal{R}_0 \to \max_{x\in\overline{\Omega}}\{\beta(x)/r(x)\}$, as $\eta \to 0$, for fixed $g_1(r^{-1}) > 0$;*
(iii) *$\mathcal{R}_0 \to \int_\Omega \beta(x)\mathrm{d}x / \int_\Omega r(x)\mathrm{d}x$, as $\eta \to \infty$, for fixed $g_1(r^{-1}) > 0$;*
(iv) *$sign(1 - \mathcal{R}_0) = sign\,\zeta^*$;*
(v) *$\min_{x\in\overline{\Omega}}\{\beta(x)/r(x)\} \le \mathcal{R}_0 \le \max_{x\in\overline{\Omega}}\{\beta(x)/r(x)\}$.*

Proof. Multiplying the first equation of (2.10) by ϕ and then integrating by parts over Ω yields

$$\zeta \int_\Omega \beta(x)\phi^2 \mathrm{d}x = \int_\Omega g(r^{-1})|\nabla\phi|^2 \mathrm{d}x + \int_\Omega r(x)\phi \mathrm{d}x.$$

Thus, we can obtain (2.11) by the classical Krein-Rutman theorem [13]. Let (ζ_0, ϕ) be a solution of the eigenvalue problem (2.10), where ϕ is the positive eigenfunction corresponding to the eigenvalue ζ_0. We first prove the uniqueness. Assume $(\hat{\zeta}_0, \hat{\phi})$ is the another solution of (2.10). Then one has

$$\begin{aligned} &\nabla \cdot (g(r^{-1}(x))\nabla\phi) - r(x)\phi + \zeta_0\beta(x)\phi = 0, && x \in \Omega, \\ &\nabla\phi \cdot \mathbf{n} = 0, && x \in \partial\Omega, \end{aligned} \tag{2.13}$$

and

$$\begin{aligned} &\nabla \cdot (g(r^{-1}(x))\nabla\hat{\phi}) - r(x)\hat{\phi} + \hat{\zeta}_0\beta(x)\hat{\phi} = 0, && x \in \Omega, \\ &\nabla\hat{\phi} \cdot \mathbf{n} = 0, && x \in \partial\Omega. \end{aligned} \tag{2.14}$$

Multiplying the first equations of (2.13) and (2.14) by $\hat{\phi}$ and ϕ respectively and then integrating by parts over Ω leads to

$$(\zeta_0 - \hat{\zeta}_0)\int_\Omega \beta(x)\phi\hat{\phi}\mathrm{d}x = 0.$$

Hence, we have $\zeta_0 = \hat{\zeta}_0$ because $\beta(\cdot)$, ϕ and $\hat{\phi}$ are positive functions. Moreover, it follows from [30, Theorem 3.2] that $\mathcal{R}_0 = 1/\zeta_0$. Similar to the proof of Lemma 2.1, we can prove (i)-(iii).

(iv) By the definition of $\mathcal{R}_0$, there exists a positive function $\phi(x) \in C^2(\overline{\Omega})$ such that

$$\begin{aligned} &\nabla \cdot (g(r^{-1}(x))\nabla\phi) - r(x)\phi + \tfrac{1}{\mathcal{R}_0}\beta(x)\phi = 0, && x \in \Omega, \\ &\nabla\phi \cdot \mathbf{n} = 0, && x \in \partial\Omega. \end{aligned} \tag{2.15}$$

Multiplying the first equations of (2.6) and (2.15) by ϕ and by ϕ^* respectively and integrating by parts over Ω yields

$$\zeta^* \int_\Omega \phi^*\phi \mathrm{d}x = \frac{1-\mathcal{R}_0}{\mathcal{R}_0} \int_\Omega \beta(x)\phi^*\phi \mathrm{d}x.$$

Since both ϕ^* and ϕ are positive functions in Ω, it follows that $\mathcal{R}_0 > 1$ if $\zeta^* < 0$, $\mathcal{R}_0 = 1$ if $\zeta^* = 0$, and $\mathcal{R}_0 < 1$ if $\zeta^* > 0$.

(v) Integrating the first equation of (2.15) over Ω gives

$$\int_\Omega r(x)\left[\mathcal{R}_0 - \frac{\beta(x)}{r(x)}\right]\phi \mathrm{d}x = 0.$$

Then (v) holds because of the positivity of $r(\cdot)$ and ϕ. This ends the proof. □

Lemma 2.3. *If $\mathcal{R}_0 < 1$, then the DEF E_0 is stable; If $\mathcal{R}_0 > 1$, then the DEF E_0 is unstable.*

Proof. (i) Suppose $\mathcal{R}_0 < 1$. We first deal with the linear stability of E_0. Let $(\overline{S}(t,x), \overline{I}(t,x)) = e^{-\zeta t}(\varphi, \phi)$. Substituting it into the linear system (2.2), one gets

$$\begin{aligned} &\nabla \cdot (f(\beta(x))\nabla\varphi) - (\beta(x) - r(x))\phi + \zeta\varphi = 0, && x \in \Omega, \\ &\nabla \cdot (g(r^{-1}(x))\nabla\phi) + (\beta(x) - r(x))\phi + \zeta\phi = 0, && x \in \Omega, \\ &\nabla\varphi \cdot \mathbf{n} = \nabla\phi \cdot \mathbf{n} = 0, && x \in \partial\Omega. \end{aligned} \tag{2.16}$$

To prove the linear stability of E_0, it suffices to show the problem (2.16) possesses a solution (ζ, φ, ϕ) for which the real part of ζ is positive, and φ or ϕ is not identically zero on Ω. Arguing by contradiction, we assume the problem (2.16) has a (ζ, φ, ϕ) satisfying the real part of ζ is nonpositive, and φ or ϕ is not identically zero on Ω. We claim $\phi(x) \not\equiv 0$ for all $x \in \Omega$. If not, then one has $\varphi(x) \not\equiv 0$ on Ω. From the first equation of (2.16), we have

$$\begin{aligned} &\nabla \cdot (f(\beta(x))\nabla\varphi) + \zeta\varphi = 0, && x \in \Omega, \\ &\nabla\varphi \cdot \mathbf{n} = 0, && x \in \partial\Omega. \end{aligned} \tag{2.17}$$

Thus, $\zeta \int_\Omega \varphi \mathrm{d}x = 0$ by integrating the above equation over Ω. This implies that $\zeta = 0$ owing to $\varphi \not\equiv 0$ on Ω. By (2.17), we see that φ is a constant, denoted by $\overline{\varphi}$. Combining with (2.1) and (2.3), one gets

$$\int_\Omega (\varphi + \phi)\mathrm{d}x = e^{\zeta t}\int_\Omega (\overline{S}(t,x) + \overline{I}(t,x))\mathrm{d}x = e^{\zeta t}\int_\Omega (S(t,x) - \tilde{S}_0 + I(t,x))\mathrm{d}x = 0. \tag{2.18}$$

Since $\phi(\cdot) \equiv 0$ on Ω, $\overline{\varphi} \equiv 0$ which contradicts with the fact $\varphi(\cdot) \not\equiv 0$ on Ω. Hence, the above claim is true. Because the operator $\nabla \cdot (g(r^{-1})\nabla) + \beta(x) - r(x)$ is self-adjoint, it follows from the second equation of (2.16) that ζ is real and nonpositive. By the definition of ζ^*, we obtain $\zeta^* \le \zeta \le 0$. However, from Lemma 2.2 (iv), $\mathcal{R}_0 \ge 1$ which is a contradiction. Therefore, the ζ has a positive real part which means that the DFE is linearly stable. Furthermore, the DFE is stable by applying the theories in [9].

(ii) Suppose $\mathcal{R}_0 > 1$. Similar to the case $\mathcal{R}_0 < 1$, to cope with the linear instability of DFE, it is only necessary to prove that there exists a solution (ζ, φ, ϕ) for (2.16) satisfying (2.18), where ζ has a negative real part and $\phi(x)$ is positive for all $x \in \Omega$. Note that ζ^* and ϕ^* satisfy (2.6) and ϕ^* is positive on Ω. Substituting (ζ^*, ϕ^*) into the first equation of (2.16), we obtain

$$\begin{aligned} &\nabla \cdot (f(\beta(x))\nabla\varphi) - (\beta(x) - r(x))\phi^* + \zeta^*\varphi = 0, && x \in \Omega, \\ &\nabla\varphi \cdot \mathbf{n} = \nabla\phi^* \cdot \mathbf{n} = 0, && x \in \partial\Omega. \end{aligned}$$

Since $\zeta^* < 0$ from Lemma 2.2 (iv), the above system admits a unique solution φ^*. Adding the two equations of (2.16) with $(\zeta^*, \phi^*, \varphi^*)$ and integrating the results equation over Ω yields

$$\zeta^* \int_\Omega (\varphi^* + \phi^*)\mathrm{d}x = 0,$$

which indicates that $\int_\Omega (\varphi^* + \phi^*)\mathrm{d}x = 0$. To sum up, the system (2.16) has a solution $(\zeta^*, \phi^*, \varphi^*)$ where $\zeta^* < 0$ and $\phi^* > 0$ for all $x \in \Omega$. Thus, the DFE is linearly unstable. According to [9], the DFE is unstable. This finishes the proof. □

Lemma 2.4. *If $\mathcal{R}_0 < 1$, then the solution $(S(t,x), I(t,x)) \to (\tilde{S}_0, 0)$ in $C(\Omega)$ as $t \to \infty$.*

Proof. By the second equation of system (1.6), we obtain

$$\begin{aligned} &I_t \le \nabla\cdot(g(r^{-1}(x))\nabla I) + (\beta(x)-r(x))I, && t>0,\ x\in\Omega,\\ &\nabla I\cdot\mathbf{n}=0, && t>0,\ x\in\partial\Omega,\\ &I(x,0)=I_0(x)\ge 0, && t=0,\ x\in\Omega. \end{aligned}$$

Define a auxiliary function $\psi(t,x) := Pe^{-\zeta^* t}\phi^*(x)$, wherein $\zeta^*>0$, $\phi^*>0$ are determined by Lemma 2.1 and P is a sufficiently large constant satisfying $\psi(0,x)\ge I(0,x)$, for any $x\in\Omega$. By direct calculations, we obtain

$$\begin{aligned} &\psi_t = \nabla\cdot(g(r^{-1}(x))\nabla\psi) + (\beta(x)-r(x))\psi, && t>0,\ x\in\Omega,\\ &\nabla\psi\cdot\mathbf{n}=0, && t>0,\ x\in\partial\Omega,\\ &\psi(0,x)\ge I(0,x)\ge 0, && t=0,\ x\in\Omega. \end{aligned}$$

By the comparison principle, $I(t,x)\le\psi(t,x)$ for all $t>0$ and $x\in\Omega$. Then $I(t,x)$ converges to zero as t tends to ∞ owing to the fact that $\psi(t,\cdot)\to 0$ when $t\to\infty$ in Ω.

Next, we will show $S(t,x)\to\tilde{S}_0$ as $t\to\infty$, $x\in\Omega$. Combining the above analysis and the facts that $\beta(x)$ and $r(x)$ are continuous functions of x, from the first equation of (1.6), there is a constant $M_1>0$ such that

$$|S_t - \nabla\cdot(f(\beta(x))\nabla S)| \le M_1 e^{-\zeta^* t},$$

for $t>0$, $x\in\Omega$. Then $|S_t-\nabla\cdot(f(\beta(x))\nabla S)|\to 0$ when $t\to\infty$, $x\in\Omega$. Thus, by using the boundary condition $\nabla S\cdot\mathbf{n}=0$ on $\partial\Omega$, one can see that $S(t,\cdot)$ converges to a positive constant as $t\to\infty$ in Ω. Set

$$S(t,x) = u_1(t) + u_2(t,x),$$

where $u_1(t) = \frac{1}{|\Omega|}\int_\Omega S(t,x)\mathrm{d}x$. By simple calculations, we obtain

$$\frac{\mathrm{d}u_1(t)}{\mathrm{d}t} = \frac{1}{|\Omega|}\int_\Omega (S_t(t,x) - \nabla\cdot(f(\beta(x))\nabla S))\mathrm{d}x,$$

which implies that there is a constant $M_2>0$ such that $|\mathrm{d}u_1(t)/\mathrm{d}t|\le M_2 e^{-\zeta^* t}$, $t>0$. Moreover, one has

$$\begin{aligned} &(u_2)_t = \nabla\cdot(f(\beta(x))\nabla u_2) + k(t,x), && t>0,\ x\in\Omega,\\ &\nabla u_2\cdot\mathbf{n}=0, && t>0,\ x\in\partial\Omega, \end{aligned}$$

where

$$k(t,x) = \Big(-\frac{\beta(x)S}{S+I} + r(x)\Big)I - \frac{\mathrm{d}u_1(t)}{\mathrm{d}t}.$$

From the above analysis, we obtain

$$|k(t,x)|\le M_3 e^{-\zeta^* t},\ \text{ for some constant } M_3>0.$$

Since $\int_\Omega (S(t,x)+I(t,x))\mathrm{d}x = N_0$ and $I(t,\cdot)\to 0$, $t\to\infty$, we have

$$u_1(t) = \frac{1}{|\Omega|}\int_\Omega S(t,x)\mathrm{d}x \to \frac{N_0}{|\Omega|} = \tilde{S}_0,\ \text{ as } t\to\infty.$$

Choose $0=\zeta^0\le\zeta^1\le\zeta^2\le\cdots$ representing the eigenvalues of Laplace operator $-\Delta$ with homogeneous Neumann boundary condition, and the corresponding normalized eigenfunctions $\{\omega_l(x) : l = 0,1,2,\cdots, x\in\Omega\}$. Then there exist two sequences of functions $b_l(t)$ and $k_l(t)$, $l=0,1,2,\cdots$, such that

$$u_2(t,x) = \sum_{l=0}^{\infty} b_l(t)\omega_l(x)\ \text{ and }\ k(t,x) = \sum_{l=0}^{\infty} k_l(t)\omega_l(x).$$

Since $|k_l(t,x)|\le M_4 e^{-\zeta^* t}$, $t>0$, $x\in\Omega$, for some $M_4>0$, it follows that there exists a $M_5>0$ such that $|b_l(t,x)|\le M_5 e^{-\zeta^{**} t}$, $t>0$, $x\in\Omega$ where $\zeta^{**} := \min\{\zeta^*,\zeta_1\}$. Hence, $u_2(t,\cdot)\to 0$ as $t\to\infty$ on Ω. Thus, $S(t,x)\to\tilde{S}_0$ as $t\to\infty$, $x\in\Omega$. This ends the proof. □

Combining with Lemmas 2.2-2.4, we have the following main results.

Theorem 2.2. *Assume (H1)-(H3) holds with fixed N_0 and $\beta(x)-r(x)$ changes sign on Ω. Then there exists a unique DFE $E_0=(\tilde{S}_0,0)$. Moreover, if $\mathcal{R}_0<1$, then the DFE is globally asymptotically stable, but if $\mathcal{R}_0>1$, then it is unstable.*

2.2. **The endemic equilibrium.** In this subsection, we show the existence of the EE for system (1.6) when $\mathcal{R}_0 > 1$. To prove this, the following lemma is needed.

Lemma 2.5. *Suppose $\mathcal{R}_0 > 1$. Then there exists an $\varepsilon_0 > 0$ such that the solution of (1.6) satisfies*

$$\liminf_{t\to\infty} \|(S(t,x), I(t,x)) - (\tilde{S}_0, 0)\|_{L^\infty(\Omega)} > \varepsilon_0 \tag{2.19}$$

uniformly for $x \in \overline{\Omega}$.

Proof. We apply the persistence theory developed by [18] and [34] to prove this result. Denote

$$Z_0 := \{\mathbf{u}_0 \in C(\overline{\Omega}) | I_0(x) \neq 0\} \text{ and } \partial Z_0 := \{\mathbf{u}_0 \in C(\overline{\Omega}) | I_0(x) = 0\},$$

where $\mathbf{u}_0 = (S_0, I_0)$. Let $\Phi(t)\mathbf{u}_0 := (S(t,\cdot), I(t,\cdot))$, $t > 0$ be the unique solution of (1.6). It is obvious to see that $\Phi(t)$ is continuous and compact. According to Proposition 2.1, the map $\Phi(t)$ is pointwisely dissipative. By utilizing [8, Theorem 3.4.8] (or [34, Theorem 1.3.7]), $\Phi(t)$ admits a compact global attractor. To end the proof, it is necessary to prove the following claims with the help of ideas [33]:

Claim 1. $\Phi(t)Z_0 \subset Z_0$. One can easily prove this owing to the strong maximum principle [25].

Let U_∂ be the maximum positive invariant set of $\Phi(t)$ in ∂Z_0, i.e., $U_\partial := \{\mathbf{u}_0 \in C(\overline{\Omega}) | \Phi(t)\mathbf{u}_0 \in \partial Z_0\}$. One can verify that $U_\partial = \partial Z_0$. Denote $\omega(\mathbf{u}_0)$ as the omega limit set of $\mathbf{u}_0$. Set

$$\overline{U}_\partial := \bigcup\nolimits_{\{\mathbf{u}_0 \in U_\partial\}} \omega(\mathbf{u}_0).$$

Claim 2. $\overline{U}_\partial = \{E_0\}$. In fact, for any $\mathbf{u}_0 \in U_\partial$, by the definition of U_∂, one has $I(t,x) = 0$, for all $x \in \Omega$, $t \geq 0$. Thus, substituting it into the system (1.6) gives

$$\begin{aligned} &S_t = \nabla \cdot (f(\beta(x))\nabla S), && t > 0,\ x \in \Omega,\\ &\nabla S \cdot \mathbf{n} = 0, && t > 0,\ x \in \partial\Omega,\\ &S(x,0) = S_0(x) \geq 0, && t = 0,\ x \in \Omega. \end{aligned}$$

Since $\int_\Omega ((S(t,x) + I(t,x)))\mathrm{d}x = N_0$, it follows that $S(t,\cdot) \to \tilde{S}_0$ uniformly in Ω as $t \to \infty$. Hence, $\overline{U}_\partial = \{E_0\}$, and then $\{E_0\}$ is an isolated and compact invariant set for $\Phi(t)$ restricted in U_∂.

Claim 3. There is an $\varepsilon_1 > 0$, independent of initial values, such that

$$\limsup_{t\to\infty} \|\Phi(t)\mathbf{u}_0 - (\tilde{S}_0, 0)\|_{L^\infty(\Omega)} > \varepsilon_1.$$

For any $\hat{\varepsilon}_1 > 0$, by contradiction, there exists a $\hat{\mathbf{u}}_0 = (\hat{S}_0(x), \hat{I}_0(x))$ such that

$$\limsup_{t\to\infty} \|\Phi(t)\hat{\mathbf{u}}_0 - (\tilde{S}_0, 0)\|_{L^\infty(\Omega)} \leq \hat{\varepsilon}_1, \tag{2.20}$$

where $\Phi(t)\hat{\mathbf{u}}_0 = (\hat{S}(t,\cdot), \hat{I}(t,\cdot))$.

Take a sufficiently small constant $\varepsilon_2 > 0$. Let $\zeta^*(\varepsilon_2)$ be the principal eigenvalue of the eigenvalue problem

$$\begin{aligned} &\nabla \cdot (g(r^{-1}(x))\nabla\tilde{\phi}^*) + \left(\beta(x)\tfrac{\tilde{S}_0-\varepsilon_2}{\tilde{S}_0} - r(x)\right)\tilde{\phi}^* + \zeta^*(\varepsilon_2)\tilde{\phi}^* = 0, && x \in \Omega,\\ &\nabla\tilde{\phi}^* \cdot \mathbf{n} = 0, && x \in \partial\Omega. \end{aligned}$$

wherein $\tilde{\phi}^*$ is the corresponding positive eigenfunction on Ω. Since $\mathcal{R}_0 > 1$, it follows from by Lemma 2.2 that $\zeta^* < 0$, here ζ^* is the eigenvalue of (2.6). Note that $\zeta^*(\varepsilon_2) \to \zeta^* < 0$ as ε_2 tends to zero. Thus, one can choose a sufficiently small ε_2 such that $\zeta^*(\varepsilon_2) < 0$. By the arbitrariness of $\hat{\varepsilon}_1$, we set $\hat{\varepsilon}_1 = \varepsilon_2$. From (2.20), there exists a $t_0^* > 0$ such that $\hat{S}(t,\cdot) \geq \tilde{S}_0 - \varepsilon_2$ and $\hat{I}(t,\cdot) \leq \varepsilon_2$, for any $t \geq t_0^*$ and $x \in \Omega$. Consequently, we have

$$\frac{\hat{S}\hat{I}}{\hat{S}+\hat{I}} \geq \frac{(\tilde{S}_0-\varepsilon_2)}{\tilde{S}_0-\varepsilon_2+\hat{I}}\hat{I} \geq \frac{(\tilde{S}_0-\varepsilon_2)}{\tilde{S}_0-\varepsilon_2+\varepsilon_2}\hat{I} = \frac{(\tilde{S}_0-\varepsilon_2)}{\tilde{S}_0}\hat{I},$$

for all $t \geq t_0^*$ and $x \in \Omega$.

Moreover, by Proposition 2.1 and strong maximum principle, there is a $\delta_0 > 0$ small enough such that $\hat{I}(t_0^*, x) \geq \delta_0\tilde{\phi}^*$. It is not difficult to verify that $\hat{I}_h(t,\cdot)$ is a supersolution of the following problem

$$\begin{aligned} &\tilde{I}_t = \nabla \cdot (g(r^{-1}(x))\nabla\tilde{I}) + \left(\beta(x)\tfrac{\tilde{S}_0-\varepsilon_2}{\tilde{S}_0} - r(x)\right)\tilde{I} = 0, && t > t_0^*,\ x \in \Omega,\\ &\nabla\tilde{I} \cdot \mathbf{n} = 0, && t > t_0^*,\ x \in \partial\Omega,\\ &\tilde{I}(t_0^*, x) = \delta_0\tilde{\phi}^*, && t = t_0^*,\ x \in= \Omega. \end{aligned} \tag{2.21}$$

Note that $\delta_0 e^{-\zeta^*(\varepsilon_2)(t-t_0^*)}\tilde{\phi}^*(\cdot)$ is a solution of (2.21) and $\zeta^*(\varepsilon_2) < 0$. Then, one has

$$\hat{I}(t,x) \geq \delta_0 e^{-\zeta^*(\varepsilon_2)(t-t_0^*)}\tilde{\phi}^*(x) \to \infty, \text{ as } t \to \infty, \text{ for any } x \in \Omega,$$

which contradicts to (2.20). Therefore, **Claim 3** is true which implies that $\{E_0\}$ is an isolated invariant set for $\Phi(t)$, and $W^S(\{E_0\}) \cap Z_0 = \emptyset$, where $W^S(\{E_0\})$ is the stable set of $\{E_0\}$ with respect to $\Phi(t)$.

Combining with **Claims 1-3** and [34, Theorem 1.3.1], $\Phi(t)$ is uniformly persistent. Accordingly, the (2.19) is true. This completes the proof. □

Remark 2.2. *Lemma 2.5 indicates that the disease will persist.*

In a summary, we have the following main conclusion.

Theorem 2.3. *Suppose (H1)-(H3) holds and $\mathcal{R}_0 > 1$. Then the system (1.6) has at least one endemic equilibrium $(S^*(x), I^*(x))$ satisfying $S^*(x)$, $I^*(x) > 0$ on Ω.*

Proof. By Lemma 2.5, the system (1.6) is uniformly persistent when $\mathcal{R}_0 > 1$. Thus, applying [34, Theorem 1.3.7] or [18, Theorem 4.7], the system (1.6) possesses at least one endemic steady state $(S^*(x), I^*(x))$ satisfying $S^*(x)$, $I^*(x) > 0$ on Ω. □

3. The epidemic model with random diffusion

The goal of this section is to investigate the existence and stability of DFE and EE for model (1.5) with random diffusion. Similar to Proposition 2.1, we have the well-posedness of (1.5).

Proposition 3.1. *The system (1.5) admits a unique positive solution $S(t,x)$ and $I(t,x)$ satisfying*

$$(S(t,x), I(t,x)) \in C^{2,1}((0,\infty)\times\overline{\Omega}) \times C^{2,1}((0,\infty)\times\overline{\Omega}).$$

Furthermore, there is a constant $\hat{C} > 0$ independent of the initial values, and $\hat{T}_0 > 0$ such that the solution $(S(t,x), I(t,x))$ satisfies

$$\|S(t,x)\|_{L^\infty(\Omega)} + \|I(t,x)\|_{L^\infty(\Omega)} \le \hat{C}, \quad \text{for all} \quad t > \hat{T}_0.$$

3.1. The disease-free equilibrium.

In this subsection, we explore the existence and stability of the DFE for system (1.5). Adding the two equations in (1.5) gives

$$(S+I)_t = \Delta(f(\beta(x))S + g(r^{-1}(x))I).$$

Then, integrating the above equality over Ω yields

$$\int_\Omega (S(t,x) + I(t,x))_t \mathrm{d}x = 0$$

because $\nabla(f(\beta(x))S)\cdot\mathbf{n} = \nabla(g(r^{-1}(x))I)\cdot\mathbf{n} = 0$ on $\partial\Omega$. Hence, for all $t \ge 0$,

$$\int_\Omega (S(t,x) + I(t,x))\mathrm{d}x = \overline{N}_0, \quad \text{for some constant } \overline{N}_0 > 0.$$

In particular, $\overline{N}_0 = \int_\Omega (S_0(x) + I_0(x))\mathrm{d}x$.

Lemma 3.1. *System (1.5) has a unique DFE*

$$\hat{E}_0 = (\hat{S}(x), 0) = \left(\frac{\overline{N}_0}{f(\beta(x))\int_\Omega \frac{1}{f(\beta(x))}\mathrm{d}x}, 0\right),$$

where $\overline{N}_0 = \int_\Omega (S_0(x) + I_0(x))\mathrm{d}x > 0$.

Proof. Suppose that $(\hat{S}(x), 0)$ is a disease-free equilibrium of system (1.5). Then, from the first equation of (1.5), we obtain $\Delta(f(\beta(x))\hat{S}(x)) = 0$. From $\nabla(f(\beta(x))S(x))\cdot\mathbf{n} = 0$, it follows that $f(\beta(x))\hat{S}(x) = C$ for some constant C. Then, $\hat{S}(x) = C/f(\beta(x))$. Moreover, according to $\int_\Omega \hat{S}(x)\mathrm{d}x = \overline{N}_0$, we have $C = \overline{N}_0/\int_\Omega (1/f(\beta(x)))\mathrm{d}x$. Thus, one gets

$$\hat{S}(x) = \frac{\overline{N}_0}{f(\beta(x))\int_\Omega \frac{1}{f(\beta(x))}\mathrm{d}x} > 0, \quad \text{for all } x \in \Omega,$$

which completes the proof. □

Lemma 3.2. *Define $g(r^{-1}(\cdot)) = \eta g_1(r^{-1}(\cdot))$, where η and g_1 are the positive constant and the $C^3(\overline{\Omega})$ function, respectively, and*

$$\lambda^* = \inf_{\Psi\in W^{1,2}(\Omega),\Psi\neq 0}\left\{\frac{\eta\int_\Omega |\nabla\Psi|^2\mathrm{d}x + \int_\Omega \frac{r(x)-\beta(x)}{g_1(r^{-1}(x))}\Psi^2\mathrm{d}x}{\int_\Omega \frac{1}{g_1(r^{-1}(x))}\Psi^2\mathrm{d}x}\right\}.$$

If $\beta(x) - r(x)$ changes sign on Ω, then
(i) *λ^* is a strictly monotonically increasing function with respect to η;*
(ii) *$\lambda^* \to \min_{x\in\overline{\Omega}}\{(r(x)-\beta(x))g_1^{-1}(r^{-1}(x))\}$ as $\eta \to 0$, for fixed g_1;*
(iii) *$\lambda^* \to \int_\Omega (r(x)-\beta(x))g_1^{-1}(r^{-1}(x))\mathrm{d}x/\int_\Omega g_1^{-1}(r^{-1}(x))\mathrm{d}x$ as $\eta \to +\infty$, for fixed g_1;*

(iv) *If* $\int_\Omega \beta(x) g_1^{-1}(r^{-1}(x))\mathrm{d}x \geq \int_\Omega r(x) g_1^{-1}(r^{-1}(x))\mathrm{d}x$ *then* $\lambda^* < 0$ *for all* $\eta > 0$*;*
(v) *If* $\int_\Omega \beta(x) g_1^{-1}(r^{-1}(x))\mathrm{d}x < \int_\Omega r(x) g_1^{-1}(r^{-1}(x))\mathrm{d}x$*, then the equation* $\lambda^*(\eta) = 0$ *has a unique positive root denoted by* $\bar{\eta}^*$*. Furthermore, if* $\eta < \bar{\eta}^*$ *then* $\lambda^* < 0$*, and if* $\eta > \bar{\eta}^*$ *then* $\lambda^* > 0$*.*

Proof. Linearizing the system (1.5) around the DFE $(\hat{S}(x), 0)$ yields

$$\begin{aligned} &\xi_t = \Delta(g(r^{-1}(x))\xi) + (\beta(x) - r(x))\xi, && t > 0,\ x \in \Omega,\\ &\nabla(g(r^{-1}(x))\xi)\cdot \mathbf{n} = 0, && t > 0,\ x \in \partial\Omega. \end{aligned}$$

Suppose that $\xi(t,x) = e^{-\lambda t}\vartheta(x)$. Then, one obtains

$$\begin{aligned} &\Delta(g(r^{-1}(x))\vartheta) + (\beta(x) - r(x))\vartheta + \lambda\vartheta = 0, && x \in \Omega,\\ &\nabla(g(r^{-1}(x))\vartheta)\cdot \mathbf{n} = 0, && x \in \partial\Omega. \end{aligned} \tag{3.1}$$

Set $\Psi(x) = g(r^{-1}(x))\vartheta(x)$. Thus, from $g(r^{-1}(\cdot)) := \eta g_1(r^{-1}(\cdot))$, system (3.1) can be reduced to

$$\begin{aligned} &\eta\Delta\Psi + \frac{(\beta(x) - r(x))}{g_1(r^{-1}(x))}\Psi + \lambda\frac{\Psi}{g_1(r^{-1}(x))} = 0, && x \in \Omega,\\ &\nabla\Psi\cdot\mathbf{n} = 0, && x \in \partial\Omega. \end{aligned} \tag{3.2}$$

Similar to the analysis of Lemma 2.1, there exists a unique eigenvalue λ^* whose corresponding eigenfunction Ψ^* is positive on Ω. Observe that (λ^*, Ψ^*) satisfies

$$\begin{aligned} &\eta\Delta\Psi^* + \frac{(\beta(x) - r(x))}{g_1(r^{-1}(x))}\Psi^* + \lambda^*\frac{\Psi^*}{g_1(r^{-1}(x))} = 0, && x \in \Omega,\\ &\nabla\Psi^*\cdot\mathbf{n} = 0, && x \in \partial\Omega. \end{aligned} \tag{3.3}$$

Therefore, λ^* is determined by the variational characterization

$$\lambda^* = \inf_{\Psi\in W^{1,2}(\Omega),\Psi\neq 0}\left\{\frac{\eta\int_\Omega |\nabla\Psi|^2\mathrm{d}x + \int_\Omega \frac{r(x)-\beta(x)}{g_1(r^{-1}(x))}\Psi^2\mathrm{d}x}{\int_\Omega \frac{1}{g_1(r^{-1}(x))}\Psi^2\mathrm{d}x}\right\},$$

after which the proof is similar to Lemma 2.1. □

To analyze the stability of the DFE $(\hat{S}(x), 0)$, we characterize the basic reproduction number $\mathcal{R}_0$ for system (1.5). Consider the following eigenvalue problem:

$$\begin{aligned} &\kappa\frac{\beta(x)}{g_1(r^{-1}(x))}\Psi = -\eta\Delta\Psi + \frac{r(x)}{g_1(r^{-1}(x))}\Psi, && x \in \Omega,\\ &\nabla\Psi\cdot\mathbf{n} = 0, && x \in \partial\Omega. \end{aligned} \tag{3.4}$$

Lemma 3.3. *Let* κ_0 *be the positive eigenvalue of* (3.4) *with a positive eigenfunction. Then* λ_0 *is unique and defined by*

$$\lambda_0 = \inf_{\Psi\in W^{1,2}(\Omega),\Psi\neq 0}\left\{\frac{\eta\int_\Omega |\nabla\Psi|^2\mathrm{d}x + \int_\Omega \frac{r(x)}{g_1(r^{-1}(x))}\Psi^2\mathrm{d}x}{\int_\Omega \frac{\beta(x)}{g_1(r^{-1}(x))}\Psi^2\mathrm{d}x}\right\}.$$

Furthermore, the basic reproduction number $\mathcal{R}_0$ *of* (1.5) *is defined by*

$$\mathcal{R}_0 = \sup_{\Psi\in W^{1,2}(\Omega),\Psi\neq 0}\left\{\frac{\int_\Omega \frac{\beta(x)}{g_1(r^{-1}(x))}\Psi^2\mathrm{d}x}{\eta\int_\Omega |\nabla\Psi|^2\mathrm{d}x + \int_\Omega \frac{r(x)}{g_1(r^{-1}(x))}\Psi^2\mathrm{d}x}\right\}.$$

Moreover, if $\beta(x) - r(x)$ *changes sign on* Ω*, then* $\mathcal{R}_0$ *satisfies the following properties:*
(i) $\mathcal{R}_0 = 1/\zeta_0$ *is monotone decreasing with respect to* η*;*
(ii) $\mathcal{R}_0 \to \max_{x\in\Omega}\{\beta(x)/r(x)\}$ *as* $\eta \to 0$*, for fixed* g_1*;*
(iii) $\mathcal{R}_0 \to \int_\Omega \beta(x) g_1^{-1}(r^{-1}(x))\mathrm{d}x / \int_\Omega r(x) g_1^{-1}(r^{-1}(x))\mathrm{d}x$ *as* $\eta \to +\infty$*, for fixed* g_1*;*
(iv) $sign(1 - \mathcal{R}_0) = sign\,\lambda^*$*;*
(v) $\min_{x\in\overline{\Omega}}\{\beta(x)/r(x)\} \leq \mathcal{R}_0 \leq \max_{x\in\overline{\Omega}}\{\beta(x)/r(x)\}$*.*

Proof. The proof follows the same logic as Lemma 2.2. □

Similar to Lemmas 2.3-2.4, we can prove the following results.

Lemma 3.4. *If* $\mathcal{R}_0 < 1$*, then the DEF* $\hat{E}_0$ *is stable; If* $\mathcal{R}_0 > 1$*, then the DEF* $\hat{E}_0$ *is unstable.*

Lemma 3.5. *If* $\mathcal{R}_0 < 1$*, then the solution* $(S(t,x), I(t,x)) \to (\hat{S}(x), 0)$ *in* $C(\Omega)$ *as* $t \to \infty$*.*

Combining with Lemmas 3.1-3.5, we have the following main results.

Theorem 3.2. *Assume (H1)-(H3) holds with fixed* N_0 *and* $\beta(x) - r(x)$ *changes sign on* Ω*. Then there exists a unique DFE* $\hat{E}_0 = (\hat{S}(x), 0)$*. Furthermore, if* $\mathcal{R}_0 < 1$*, then the DFE is globally asymptotically stable, but if* $\mathcal{R}_0 > 1$*, then it is unstable.*

3.2. **The endemic equilibrium.** In this subsection, we explore the existence of the EE for system (1.5) when $\mathcal{R}_0 > 1$. The steady states of (1.5) satisfy

$$\begin{aligned} &\Delta(f(\beta(x))S) - \Big(\tfrac{\beta(x)S}{S+I} - r(x)\Big)I = 0, && x \in \Omega,\\ &\Delta(g(r^{-1}(x))I) + \Big(\tfrac{\beta(x)S}{S+I} - r(x)\Big)I = 0, && x \in \Omega,\\ &\nabla(f(\beta(x))S)\cdot\mathbf{n} = \nabla(g(r^{-1}(x))I)\cdot\mathbf{n} = 0, && x \in \partial\Omega. \end{aligned} \tag{3.5}$$

Then it follows that

$$\begin{aligned} &f(\beta(x))S + g(r^{-1}(x))I = \mu, && x \in \Omega,\\ &\Delta(g(r^{-1}(x))I) + \left(\beta(x) - r(x) - \tfrac{\beta(x)I}{S+I}\right)I = 0, && x \in \Omega,\\ &\nabla(f(\beta(x))S)\cdot\mathbf{n} = \nabla(g(r^{-1}(x))I)\cdot\mathbf{n} = 0, && x \in \partial\Omega,\\ &\int_\Omega (S+I)dx = \overline{N}_0, \end{aligned} \tag{3.6}$$

for some constant $\mu > 0$. Set

$$u = \frac{f(\beta(x))S}{\mu} \quad \text{and} \quad v = \frac{g(r^{-1}(x))I}{\mu}.$$

Substituting it into (3.6) gives

$$\begin{aligned} &u + v = 1, && x \in \Omega,\\ &\Delta v + \mathcal{K}(x,v)v = 0, && x \in \Omega,\\ &\nabla v\cdot\mathbf{n} = 0, && x \in \partial\Omega,\\ &\mu = \overline{N}_0 \cdot \left[\int_\Omega \left(\frac{u}{f(\beta(x))} + \frac{v}{g(r^{-1}(x))}\right)dx\right]^{-1}, \end{aligned} \tag{3.7}$$

where

$$\mathcal{K}(x,v) = \frac{1}{g(r^{-1}(x))}\left(\beta(x) - r(x) - \frac{\beta(x)f(\beta(x))v}{g(r^{-1}(x))(1-v) + f(\beta(x))v}\right).$$

Clearly, if (u,v) is a positive solution of (3.7), then $\left(\frac{\mu u}{f(\beta(x))}, \frac{\mu v}{g(r^{-1}(x))}\right)$ is the EE of (1.5).

Lemma 3.6. *Assume $\mathcal{R}_0 > 1$. Then system (3.7) admits a nonnegative solution (u,v) satisfying $u(\cdot), v(\cdot) \in C^2(\overline{\Omega})$ and $v(\cdot) \not\equiv 0$ on Ω. Furthermore, the solution is unique, $u(x) > 0$, and $0 < v(x) < 1$ for all $x \in \Omega$.*

Proof. Define $\mathcal{H}(v) := \Delta v + \mathcal{K}(x,v)v$. Then, by (3.7) we obtain

$$\begin{aligned} &\mathcal{H}(v) = 0, && x \in \Omega,\\ &\nabla v\cdot\mathbf{n} = 0, && x \in \partial\Omega. \end{aligned} \tag{3.8}$$

In the following, we show that there is a sufficiently small constant $\sigma > 0$ such that $\underline{v}(x) = \sigma\Psi^*(x)$ and $\overline{v}(x) \equiv 1$ are the sub- and super-solutions of system (3.8), respectively, where Ψ^* is the eigenfunction of the corresponding eigenvalue λ^* of system (3.3). By Lemma 3.3, $\lambda^* < 0$ because of $\mathcal{R}_0 > 1$. Denote

$$\mathcal{K}_1(x,v) = \frac{f(\beta(x))v}{g(r^{-1}(x))(1-v) + f(\beta(x))v}.$$

It is easy to see $\partial_v\mathcal{K}_1(x,v) > 0$, for any $x \in \Omega$. That is, $\mathcal{K}_1(x,v)$ is an increasing function of v and $\mathcal{K}_1(\cdot,v) \in [0,1]$ as $v \in [0,1]$. According to (3.3) and (3.8), we obtain

$$\mathcal{H}(\underline{v}) = \frac{\sigma\Psi^*}{g(r^{-1}(x))}[-\lambda^* - \beta(x)\mathcal{K}_1(x,\sigma\Psi^*)].$$

Since $\mathcal{K}_1$ is increasing and $\mathcal{K}_1(x,0) = 0$, it follows from the continuity of $\mathcal{K}_1$ that there exists a $\sigma > 0$ sufficiently small so that $\beta(x)\mathcal{K}_1(x,\sigma\Psi^*) < -\lambda^*$ owing to the positivity of $\beta(x)$. Hence, $\mathcal{H}(\underline{v}) > 0$ for sufficiently small $\sigma > 0$. By $\nabla\underline{v}\cdot\mathbf{n} = 0$ on $\partial\Omega$, we can see that $\underline{v}(x) = \sigma\Psi^*(x)$ is a sub-solution of (3.8). Moreover, by direct calculations, we have $\mathcal{H}(\overline{v}) = -r(x)/g(r^{-1}(x)) < 0$, $x \in \Omega$ and $\nabla\overline{v}\cdot\mathbf{n} = 0$, $x \in \partial\Omega$. This indicates that $\overline{v}(x) \equiv 1$ is a super-solution of (3.8). For a sufficiently small $\sigma > 0$, $\underline{v} < \overline{v}$ holds. By the definition of sub-and super-solution [27], one has $\underline{v}(x) \le v(x) \le \overline{v}(x)$, $x \in \Omega$. Thus, the solutions of (3.8) satisfy $0 < v(x) \le 1$ on Ω. To prove $v(x) < 1$ on Ω, by contradiction, we assume $v(x_0) = 1$ for some $x_0 \in \Omega$. Then $\Delta v(x_0) \le 0$ due to the fact $v(x_0) = \max_{x\in\Omega} v(x)$. Hence, we have

$$0 = \mathcal{H}(v(x_0)) = \Delta v(x_0) - \frac{r(x)}{g(r^{-1}(x))} < 0,$$

which is a contradiction. Therefore, $0 < v(x) < 1$ on Ω.

To cope with the uniqueness of v, we suppose that the system (3.8) has two pairs of solutions, denoted by (u^1,v^1) and (u^2,v^2), satisfying $v^1 \not\equiv v^2$. From the first equation of (3.7), one has $0 < v^1, v^2 \le 1$, $x \in \Omega$. According to the strong maximum principle [25], $0 < v^1, v^2 \le 1$, $x \in \overline{\Omega}$. From the above analysis, we have $\underline{v} \le v^1(x), v^2(x) \le \overline{v}$, $x \in \overline{\Omega}$. Let $v^a(x)$ and $v^b(x)$ be the minimal and maximal solutions of (3.8) satisfying

$v^a \not\equiv v^b$. Clearly, $\sigma\Psi^* \le v^a, v^b \le 1$, $x \in \overline{\Omega}$. Due to $v^1 \not\equiv v^2$, then $v^a \le v^b$ with $v^a \not\equiv v^b$. Applying the strong maximum principle yields that $v^a(x) < v^b(x)$, $x \in \overline{\Omega}$. Substituting v^a and v^b into (3.8), we obtain

$$\begin{aligned} &\Delta v^a + \mathcal{K}(x, v^a)v^a = 0, && x \in \Omega, \\ &\nabla v^a \cdot \mathbf{n} = 0, && x \in \partial\Omega, \end{aligned} \tag{3.9}$$

and

$$\begin{aligned} &\Delta v^b + \mathcal{K}(x, v^b)v^b = 0, && x \in \Omega, \\ &\nabla v^b \cdot \mathbf{n} = 0, && x \in \partial\Omega. \end{aligned} \tag{3.10}$$

Multiplying the equations of (3.9) and (3.10) by v^b and v^a, respectively, and integrating by parts over Ω and then subtracting the resulting equations, one obtains

$$\int_\Omega [\mathcal{K}(x, v^a) - \mathcal{K}(x, v^b)]v^a v^b \mathrm{d}x = 0.$$

On the other hand, it is not difficult to verify $\mathcal{K}(\cdot, v)$ is a decreasing function of v for any $x \in \Omega$. Thus, $\mathcal{K}(x, v^a) > \mathcal{K}(x, v^b)$ for $x \in \Omega$. Therefore,

$$\int_\Omega [\mathcal{K}(x, v^a) - \mathcal{K}(x, v^b)]v^a v^b \mathrm{d}x > 0,$$

due to $v^a, v^b > 0$. This is a contradiction. Consequently, system (3.8) admits a unique solution (u, v) satisfying $u(x) > 0$ and $0 < v(x) < 1$ for all $x \in \Omega$. □

By Lemma 3.6, we have the following conclusion.

Theorem 3.3. *Suppose $\mathcal{R}_0 > 1$. Then system (3.5) admits a nonnegative solution $(S^*(x), I^*(x))$ satisfying $S^*, I^* \in C^2(\overline{\Omega})$ and $I \not\equiv 0$ on Ω. Furthermore, the solution is unique, $S^*(x) > 0$, and $I^*(x) > 0$ for $x \in \Omega$, and given by the following formula:*

$$(S^*(x), I^*(x)) = \left(\frac{\mu u(x)}{f(\beta(x))}, \frac{\mu v(x)}{g(r^{-1}(x))} \right),$$

where $u(\cdot)$ and $v(\cdot)$ are defined in Lemma 3.6.

Remark 3.1. *If the diffusion rates $f(\beta)$ and $g(r^{-1})$ are constants in the systems (1.5) and (1.6), the relevant results belong to the special case that was analyzed in [1].*

4. Numerical computations for threshold dynamics

We first verify the threshold dynamics on the basic reproduction number $\mathcal{R}_0$ by numerical simulations. Our theoretical results will be verified numerically by choosing functions $\beta(\cdot)$, $r(\cdot)$, $f(\beta(\cdot))$ and $g(r^{-1}(\cdot))$. Specifically, (i) we study the threshold dynamics of systems (1.5) and (1.6) by testing two cases with $\mathcal{R}_0 < 1$ and $\mathcal{R}_0 > 1$; (ii) in order to discuss how the spatial heterogeneity and the motility of infected populations affect disease dynamics, we investigate the effects of $\mathcal{R}_0$ on the transmission rate $\beta(x)$ and the diffusion rate $g(x)$. For convenience, we consider a one-dimensional space.

4.1. Threshold dynamics of system (1.6).

In this subsection, we test the variation of basic reproduction number $\mathcal{R}_0$ for system (1.6) on β and g, and explore the dynamics of (1.6). For numerical examples, we take

$$\beta(x) = 1.7 - c_1^2 x,\ r(x) = 1 + x,\ f(\beta(x)) = \beta(x) \text{ and } g(r^{-1}(x)) = \eta r^{-1}(x), \tag{4.1}$$

and compute the basic reproduction number $\mathcal{R}_0$ for $0 < c_1 < 1$ and $0 < \eta < 10$. From Fig. 2(a), it follows that $\mathcal{R}_0$ is a decreasing function of c_1 and $\mathcal{R}_0 < 1$ when $c_1 > 0.65$, which implies that we should take necessary isolation measures to make $c_1 > 0.65$ to control the spread of disease. From Fig. 2(b), we see that $\mathcal{R}_0$ is a decreasing function of η. More precisely, $\mathcal{R}_0 \to 1.67379 \approx \max_{0<x<1}\{\beta(x)/r(x)\}$ as $\eta \to 0$ and $\mathcal{R}_0 \to 0.803514 \approx \int_0^1 \beta(x)\mathrm{d}x / \int_0^1 r(x)\mathrm{d}x$ as $\eta \to 10$, which demonstrate the results in Lemma 2.2.

For the case with $c_1 = 1$ and $\eta = 1$, we can easily compute $\mathcal{R}_0 = 0.8322 < 1$. By considering one unit of spatial length as one kilometer, we choose the initial densities $S_0(x) = 999$ and $I_0(x) = 1$, $x \in (0, 1)$. The solution is given in Fig. 3 for the case $\mathcal{R}_0 < 1$. The infected population tends to zero globally and the susceptible population tends to $\tilde{S}_0 = 1000$, which is consistent with Theorem 2.2.

Next, we choose $\beta(x) = 3 - x$ with other parameters in (4.1) unchanged. Then, we obtain $\mathcal{R}_0 = 1.7008 > 1$ and the solution is given in Fig. 4. The system (1.6) admits an endemic equilibrium when $\mathcal{R}_0 > 1$. This indicates that the disease will persist.

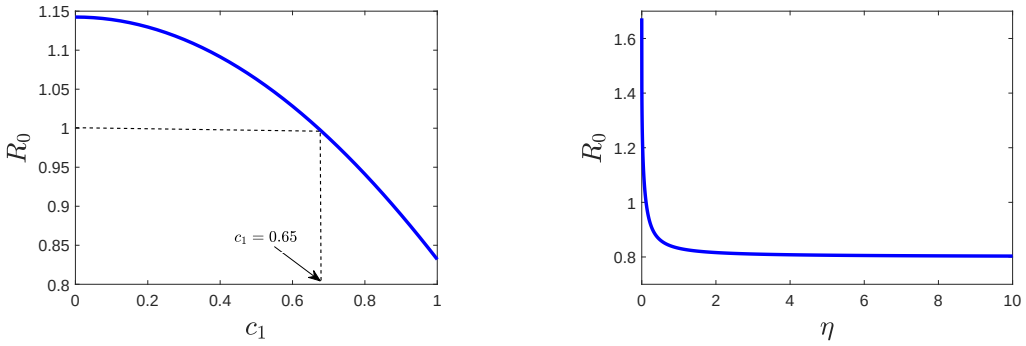

(a) (b)

FIGURE 2. (a) $\mathcal{R}_0$ vs c_1 when $\beta(x) = 1.7 - c_1^2 x$, $r(x) = 1 + x$, $f(\beta(x)) = \beta(x)$ and $g(r^{-1}(x)) = r^{-1}(x)$, $x \in [0, 1]$; (b) $\mathcal{R}_0$ vs η when $\beta(x) = 1.7 - x$, $r(x) = 1 + x$, $f(\beta(x)) = \beta(x)$ and $g(r^{-1}(x)) = \eta r^{-1}(x)$, $x \in [0, 1]$.

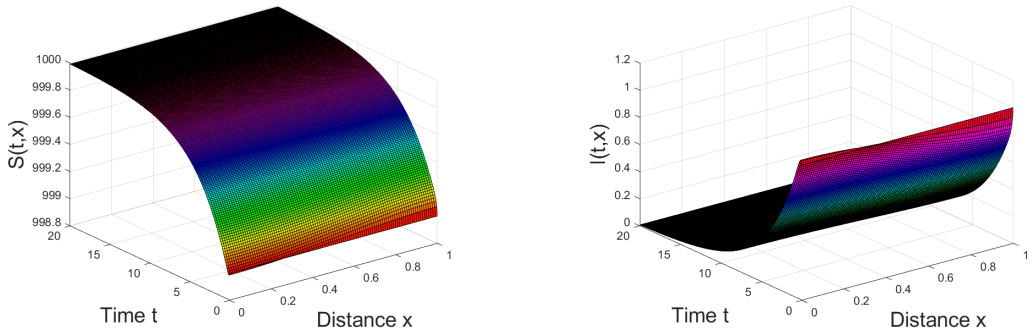

(a) (b)

FIGURE 3. The dynamics of susceptible and infected populations when $\mathcal{R}_0 = 0.8322 < 1$. (a) $S(t, x)$; (b) $I(t, x)$.

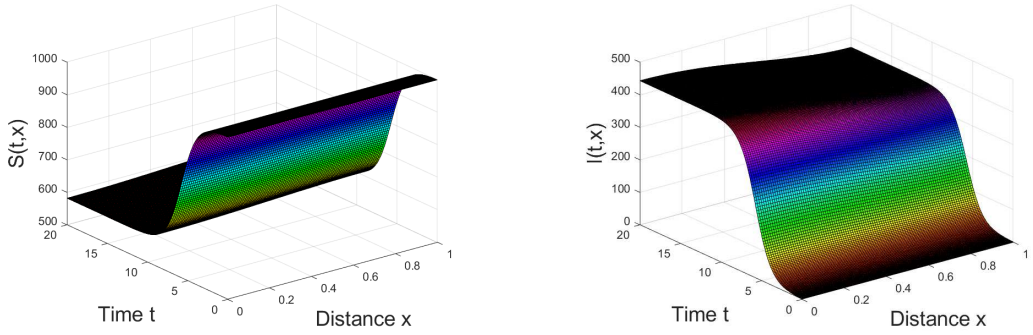

(a) (b)

FIGURE 4. The dynamics of susceptible and infected populations when $\mathcal{R}_0 = 1.7008 > 1$. (a) $S(t, x)$; (b) $I(t, x)$.

4.2. **Threshold dynamics of system (1.5).** In this subsection, we test the variation of basic reproduction number $\mathcal{R}_0$ for system (1.5) on β and g, and explore the dynamics of (1.5). For numerical examples, we take the same parameter values in (4.1).

We sketch the graphs of $\mathcal{R}_0$ for the system (1.5). In this model, we still have that $\mathcal{R}_0$ is a decreasing function of c_1 and η. The main difference in using a different diffusion law is the size of the reproduction number. Fig. 5(a) shows that $\mathcal{R}_0 < 1$ when $c_1 > 0.54$, which is smaller than the critical value $c_1 = 0.65$ of Fickian case. Fig. 5(b) shows that $\mathcal{R}_0$ is a decreasing function of η and $\mathcal{R}_0 \to 1.67379 \approx \max_{0<x<1}\{\beta(x)/r(x)\}$ as $\eta \to 0$ and $\mathcal{R}_0 \to 0.7398 \approx \int_0^1 \beta(x)g_1^{-1}(r^{-1}(x))\mathrm{d}x / \int_0^1 r(x)g_1^{-1}(r^{-1}(x))\mathrm{d}x$ as $\eta \to 10$ (see Lemma 3.3). Note that the limit as $\eta \to 0$ is same as Fickian case and the limit as $\eta \to 10$ is smaller than Fickian case.

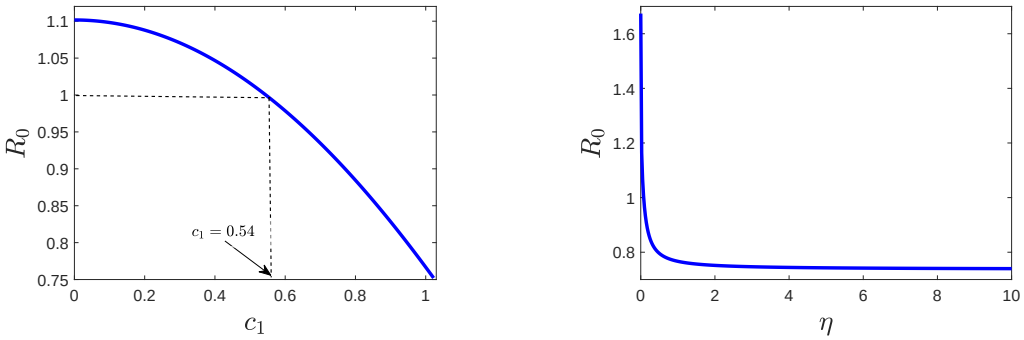

(a) (b)

FIGURE 5. (a) $\mathcal{R}_0$ vs c_1 when $\beta(x) = 1.7 - c_1^2 x$, $r(x) = 1 + x$, $f(\beta(x)) = \beta(x)$ and $g(r^{-1}(x)) = r^{-1}(x)$, $x \in [0, 1]$; (b) $\mathcal{R}_0$ vs η when $\beta(x) = 1.7 - x$, $r(x) = 1 + x$, $f(\beta(x)) = \beta(x)$ and $g(r^{-1}(x)) = \eta r^{-1}(x)$, $x \in [0, 1]$.

In the following, we investigate the threshold dynamics for system (1.5). Without loss of generality, we fix $c_1 = 1$ and $\eta = 1$ in (4.1). By direct calculations, we obtain $\mathcal{R}_0 = 0.7667 < 1$. Moreover, we assume the initial densities $S_0(x) = 999$ and $I_0(x) = 1$, $x \in (0, 1)$. Therefore, Fig. 6 presents the corresponding long term behavior of system (1.5) in the case of $\mathcal{R}_0 = 0.746021 < 1$. From Fig. 6, one can see that the number of infectives tends to zero and the number of susceptibles tends to the steady state level $\hat{S}(x) = \frac{1000}{(1.7-x)(\ln 17 - \ln 7)}$, which coincides with Theorem 3.2.

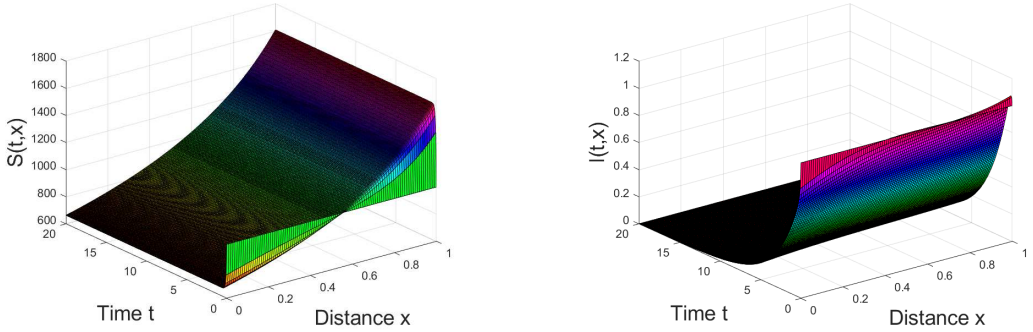

(a) (b)

FIGURE 6. The dynamics of susceptible and infected populations when $\mathcal{R}_0 = 0.7667 < 1$. (a) $S(t, x)$; (b) $I(t, x)$.

In addition, we choose $\beta(x) = 3 - x$ and other parameter values are the same as Fig. 6. Then, we have $\mathcal{R}_0 = 1.60408 > 1$. Hence, Fig. 7 shows the corresponding long term behavior of system (1.5) when $\mathcal{R}_0 = 1.60408 > 1$. From Fig. 7, system (1.5) admits an endemic equilibrium when $\mathcal{R}_0 > 1$. This implies a disease outbreak.

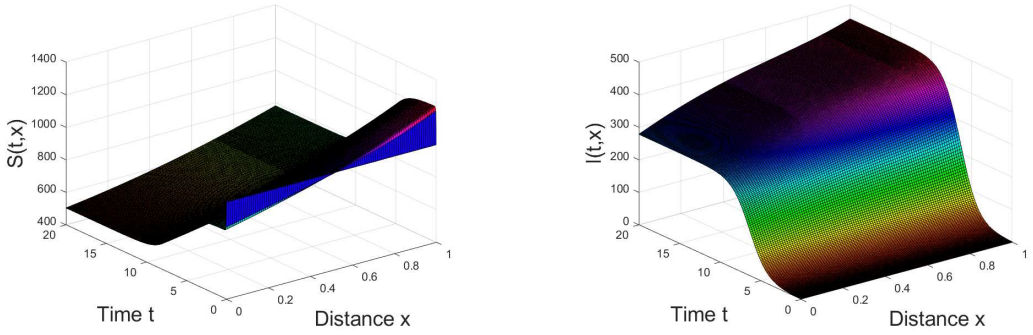

(a) (b)

FIGURE 7. The evolution of susceptible and infected human when $\mathcal{R}_0 = 1.60408 > 1$. (a) The evolution of $S(t,x)$; (b) The evolution of $I(t,x)$.

5. Numerical computations for segregation impacted by cognitive dispersal strategies

Disease spread in an ODE model means an increase in the number of infections under the well-mixed assumption, but not spatial spread. The PDE model used in the paper is to quantify the spatial spread of disease, where diffusion models the average spatial movement of individuals. In this section, we consider three examples of transmission and recovery rates, $\beta(x)$ and $r(x)$, to numerically test the impact of diffusion on the spatial spread of an infectious disease. In the first example, we will see that the heterogeneous random diffusion in the reaction-diffusion system (1.5) may segregate infected and susceptible populations and reduce the infected population. In the second example, random diffusion may reduce the infected population by using disease-free regions even if it reduces the segregation indices. In the third example, we will see that random diffusion may increase the infected population in certain situations. On the other hand, symmetric diffusion in (1.6) behaves similarly as the homogeneous diffusion with constant diffusivity.

5.1. **Example 1** (Segregation by dispersal). It is generally believed that the diffusion mechanism homogenizes a mixture of substances and reduces the segregation of substances. The reason for such a belief is from the nature of symmetric diffusion models. However, heterogeneous random diffusion models may segregate different substances. In the first example, we will see that an epidemic model with random diffusion may segregate the susceptible and the infected populations, and reduce the proportion of the infected population. The infection and the recovery rates of the first example are taken as

$$\beta(x) = 6\cos x + 6.6, \quad r(x) = \cos x + 1.5, \quad x \in \Omega = (0, 2\pi).$$

The graphs of these two rates are given in Fig. 8(a). This is an example that the patterns for $\beta(x)$ and $r(x)$ are similar, where the two have critical points at the same location. The diffusion rates are given by relations

$$f(x) = \beta(x) \quad \text{and} \quad g(x) = r^{-1}(x),$$

where their graphs are given in Fig. 8(b). As we observe from the figure, the diffusion rate of the susceptible population is the highest whereas the diffusion rate of the infected population is the lowest. This situation may give extra segregation phenomenon caused by the diffusion, which will be observed in the simulations. We assume the diffusivity of the infected population is considerably smaller than the one of susceptible population.

To compare the segregation effects of different models, we first consider a model without diffusion:

$$\begin{aligned} &S_t = -\Big(\tfrac{\beta(x)S}{S+I} - r(x)\Big)I, && t>0,\ x\in\Omega,\\ &I_t = \Big(\tfrac{\beta(x)S}{S+I} - r(x)\Big)I, && t>0,\ x\in\Omega,\\ &S(x,0) = S_0(x) \ge 0,\ I(x,0) = I_0(x) \ge 0, && t=0,\ x\in\Omega. \end{aligned} \tag{5.1}$$

We will compare steady state solutions by solving the initial value problem for $t > 0$ large enough starting from the initial densities:

$$S_0(x) = I_0(x) = 500, \quad x \in \Omega = (0, 2\pi).$$

Note that (5.1) is an ODE model and the steady state is decided algebraically by

$$S(x) = \frac{r(x)}{\beta(x) - r(x)} I(x), \quad S(x) + I(x) = I_0(x) + S_0(x) = 1000,$$

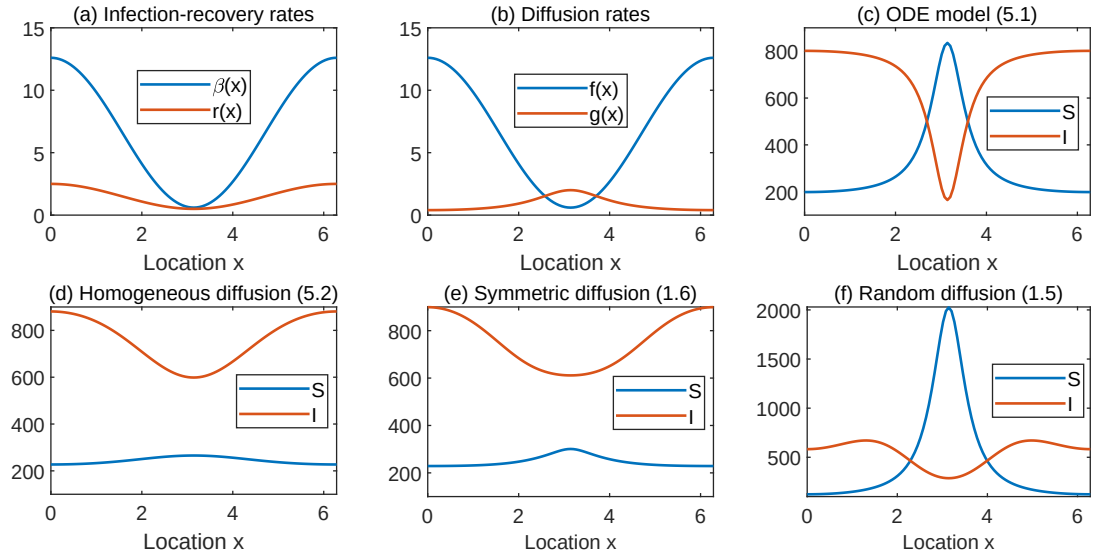

FIGURE 8. Example 1 at time $t = 50$. The infection and recovery rates have similar patterns in this example. The random diffusion segregates the two population groups and reduces the infected population.

or $I(x) = 0$ and $S(x) = 1000$. The distribution of the steady state is given in Fig. 8(c). In this figure, the susceptible and infected populations are segregated due to the heterogeneity of the ratio $\frac{r(x)}{\beta(x)-r(x)}$. There are more susceptibles in a region if the ratio is large in the region and there are fewer otherwise.

Next, we compare the effects of diffusion models. The infected population will increase if the susceptible and infected populations are mixed and will decrease if the two are segregated. For comparison, we consider the homogeneous diffusion model:

$$\begin{aligned} &S_t = d_S\Delta S + I\Big(-\tfrac{\beta(x)S}{S+I} + r(x)\Big), && t>0,\ x\in\Omega,\\ &I_t = d_I\Delta I + I\Big(\tfrac{\beta(x)S}{S+I} - r(x)\Big), && t>0,\ x\in\Omega,\\ &d_S\nabla S\cdot\mathbf{n} = 0 = d_I\nabla I\cdot\mathbf{n}, && t>0,\ x\in\partial\Omega,\\ &S(x,0) = S_0(x)\ge 0,\ I(x,0) = I_0(x)\ge 0, && t=0,\ x\in\Omega, \end{aligned} \tag{5.2}$$

where the diffusivity coefficients d_S and d_I are taken as the average diffusivity

$$d_S = \frac{1}{|\Omega|}\int_\Omega f(x)\mathrm{d}x, \quad d_I = \frac{1}{|\Omega|}\int_\Omega g(x)\mathrm{d}x.$$

The distribution of the steady state of the homogeneous diffusion model is given in Fig. 8(d). The susceptible and infected populations are more mixed. As a result, the infection fraction increases. It is not surprising that homogeneous diffusion increases infection.

Figs. 8(e)-(f) plot the distribution of the steady state of the two heterogeneous diffusion models (1.6) and (1.5), respectively. The epidemic model (1.6) with symmetric diffusion shows a similar behavior as the model (5.2) with the homogeneous diffusion. The difference is in the pointing shape of the distribution of the susceptible population, but the overall size is quite similar. On the other hand, the model (1.5) with random diffusion shows a different behavior. We can observe that the segregation index (SI) between the two populations increases and the size of the infected population decreases.

TABLE 1. The infection fraction of Example 1 with segregation indices.

Epidemic models	$\frac{\int_0^{2\pi} I\mathrm{d}x}{\int_0^{2\pi}(S+I)\mathrm{d}x}$ at $t=50$	SI-κ	SI-χ ($\times 10^5$)
ODE model (5.1)	0.6890	0.4860	-4.0474
Homogeneous diffusion (5.2)	0.7563	0.5125	2.1772
Symmetric diffusion (1.6)	0.7523	0.5046	2.0808
Random diffusion (1.5)	0.5439	0.5272	-8.8516

In Table 1, the infection fraction at the steady state of each model is compared with the segregation indices κ and χ. The two models with homogeneous or symmetric diffusion have positive segregation

indices $\chi(S,I)$, which implies that the two populations are poorly segregated and κ does not mean much for the two cases. The model with random diffusion and the ODE model have negative segregation indices $\chi(S,I)$. The index κ is larger for the random diffusion model. This implies that the random diffusion segregates the two population groups. We can also see that the infection fraction is the smallest when random diffusion is used.

5.2. **Example 2** (Dispersal toward disease-free region). Dispersal of infected individuals toward susceptible ones usually increases the infected population. However, if the dispersal is toward a region with a small basic reproduction number $\mathcal{R}_0$, dispersal may help to mitigate the disease. The second example is for such a case, where the infection and recovery rates are given by

$$\beta(x) = -4x + 5, \quad r(x) = 4x + 1, \quad x \in \Omega = (0,1). \tag{5.3}$$

The graphs of these two rates are given in Fig. 9(a). This is an example that the two rates $\beta(x)$ and $r(x)$ have the opposite monotonicity and intersect at $x = 0.5$. The diffusion rates are given by relations $f(x) = \beta(x)$ and $g(x) = r^{-1}(x)$, where the two diffusion rates have the same monotonicity as we can see from their graphs given in Fig. 9(b). Hence, the diffusion pushes both populations to the same direction. The diffusivity of the infected population is considerably smaller than the one of the susceptible population as we assumed earlier. The random diffusion will not give extra segregation effect since f and g have the same monotonicity.

The steady states of the four models are given in Fig. 9(c)–(f). We can see that only the populations of the ODE model are segregated. However, the size of the infected population is the largest in this case.

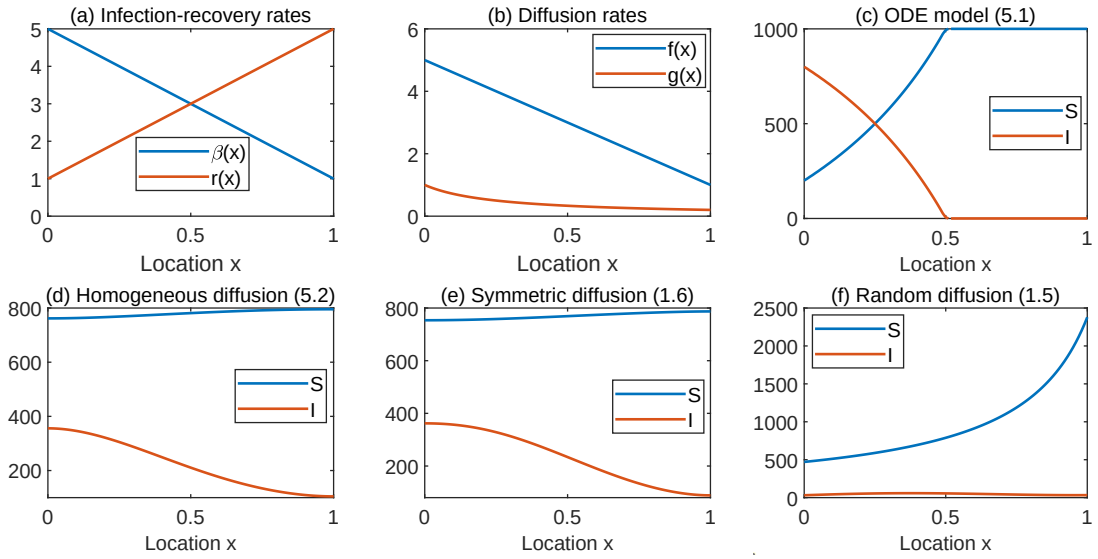

FIGURE 9. Example 2 with (5.3) at time $t = 50$. The domain $x > 0.5$ is the disease-free region for ODE model. The random diffusion pushes both populations toward the disease-free region and reduces the infected population.

To compare the segregation effects of the previous four models, we compute the steady states for the four models numerically. Figs. 9(c)–(f) plot the distribution of the steady states of the four models. We can see that the epidemic model (1.6) with symmetric diffusion shows the same behavior again as the model (5.2) with homogeneous diffusion. However, the solution of (1.5) shows a different behavior again. In particular, the size of the infected population is far smaller than the ones of other three models.

TABLE 2. The infection fraction of Example 2 with segregation indices.

Epidemic models	$\frac{\int_0^1 I\,dx}{\int_0^1 (S+I)\,dx}$ at $t = 50$	SI-κ	SI-χ ($\times 10^6$)
ODE model (5.1)	0.2355	0.6946	-0.6002
Homogeneous diffusion (5.2)	0.2201	0.5598	0.2805
Symmetric diffusion (1.6)	0.2304	0.5392	0.2735
Random diffusion (1.5)	0.0459	0.9082	1.0311

To quantitatively compare the difference of the four cases, the infection fractions are given in Table 2 with the two segregation indices. In this example, the three models with diffusion have positive segregation indices $\chi(S,I)$, which means that the three cases are not segregated. Only the ODE model has negative segregation index $\chi(S,I)$. However, the first three models have similar sizes of the infected population and only the solution of (1.5) with random diffusion has a small size of infections. The reason is that (1.5) is the only model that takes the advantage of the region $x > 0.5$ which has the disease-free equilibrium for ODE model. In conclusion, we claim that segregation is not the only way to reduce the infection but an appropriate dispersal can reduce the infection depending on the situation.

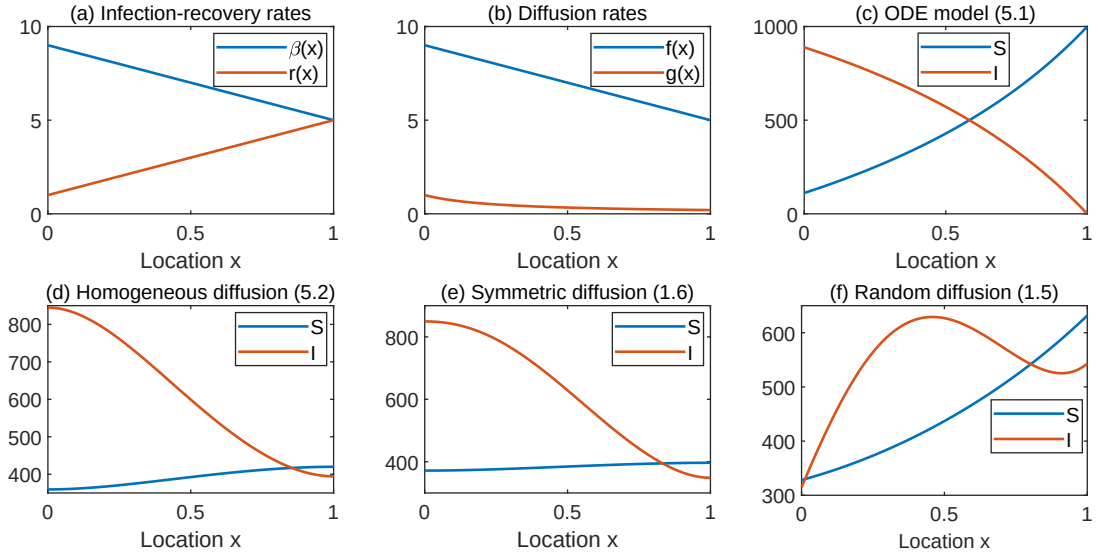

FIGURE 10. Modified Example 2 with (5.4) at time $t = 50$. If there is no disease-free region as in this example, the advantage of diffusion models disappears.

To check whether the small infected population size under the random diffusion is caused by the disease-free region of the ODE model, we modify Example 2 and remove the disease-free region by taking

$$\beta(x) = -4x + 9, \quad r(x) = 4x + 1, \quad x \in \Omega = (0,1). \tag{5.4}$$

Then, $\beta(x) > r(x)$ for all $x \in \Omega$ and the steady state of (5.1) is positive for all $x \in \Omega$. Fig. 10 plots the graphs of the steady states of the four models. The solution patterns are similar to the ones in Fig. 9. The main difference is the size of the infected population. The ODE model has the smallest infected population among all models. The homogeneous diffusion model shows a similar solution behavior as the symmetric diffusion model again.

TABLE 3. The infection fraction of modified Example 2 with segregation indices.

Epidemic models	$\frac{\int_0^1 I\,dx}{\int_0^1 (S+I)\,dx}$ at $t = 50$	SI-κ	SI-χ ($\times 10^5$)
ODE model (5.1)	0.5297	0.4423	-7.7078
Homogeneous diffusion (5.2)	0.6089	0.2230	-0.1236
Symmetric diffusion (1.6)	0.6155	0.2419	-0.2303
Random diffusion (1.5)	0.5483	0.1191	-0.1927

The infection fraction and the two segregation indices of the modified Example 2 are given in Table 3. In this example, the three models with diffusion have negative segregation indices $\chi(S,I)$, which is quite small in magnitude. We claim that the segregation of the two population groups is weak in this case. Only the ODE model has a meaningful negative segregation index $\chi(S,I)$. The sizes of the infected population of the two models with symmetric and homogeneous diffusions are larger than other two cases.

5.3. **Example 3** (Dispersal toward endemic region). We assume that the susceptible individuals intend to leave an area with a high transmission rate and the infected individuals intend to stay in an area with a high recovery rate. Under this assumption, the diffusivity is given by relations $f(x) = \beta(x)$ and $g(x) = r^{-1}(x)$. This natural assumption may give a better chance to reduce the infected population. In fact, in the previous examples, the heterogeneous random diffusion model gives the smallest infection fraction among all diffusion models. However, such a performance is not guaranteed and, in Example 3, we will see the heterogeneous random diffusion increases the infected population. We take the infection and recovery rates as

$$\beta(x) = 5e^{-160(x-0.15)^2} + 2, \quad r(x) = 8e^{-160(x-0.85)^2} + 1, \quad x \in \Omega = (0, 1).$$

The graphs are given in Fig. 11(a). In this example, $\beta(x)$ and $r(x)$ have maximum points apart. The diffusion rates are given by relations $f(x) = \beta(x)$ and $g(x) = r^{-1}(x)$ and their graphs are given in Fig. 11(b). In this example, the diffusion rate of the susceptible population is highest at $x = 0.15$ and the diffusion rate of the infected population is lowest at $x = 0.85$.

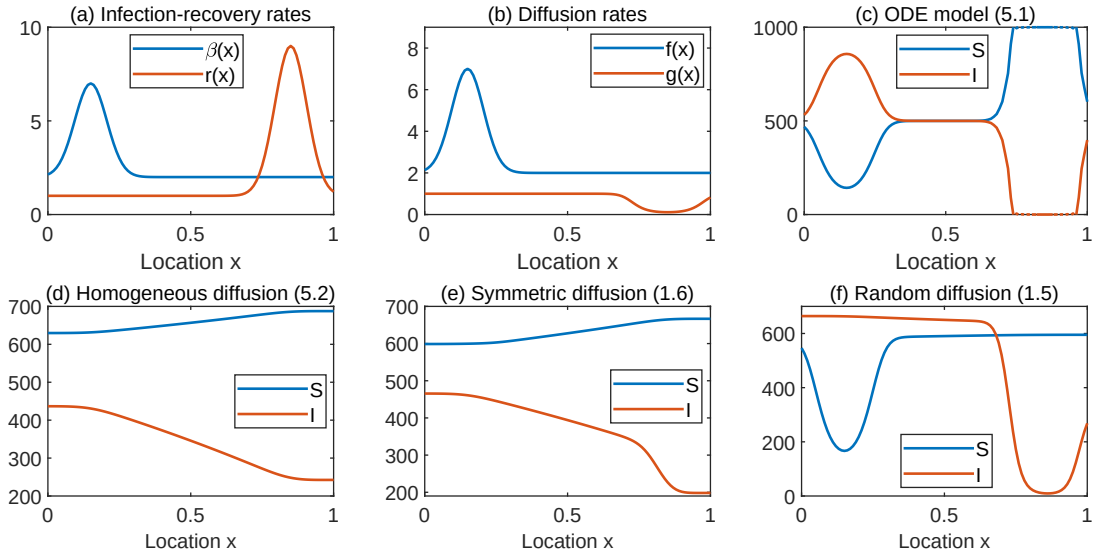

FIGURE 11. Example 3 at time $t = 50$. The maxima of infection and recovery rates are placed apart in this example. The segregation of the two populations does not help to reduce the infected population in this case.

The steady states of the four models are computed numerically and given in Figs. 9(c)–(f). We can see that the model (1.6) with symmetric diffusion shows the similar behavior as the model (5.2) with homogeneous diffusion. However, the solution behavior of the random diffusion model (1.5) is different but partially similar to the one of the ODE model.

TABLE 4. The infection fraction of of Example 3 with segregation indices.

Epidemic models	$\frac{\int_0^1 I\mathrm{d}x}{\int_0^1 (S+I)\mathrm{d}x}$ at $t = 50$	SI-κ	SI-χ ($\times 10^5$)
ODE model (5.1)	0.4340	0.4048	-7.3444
Homogeneous diffusion (5.2)	0.3421	0.3158	0.8594
Symmetric diffusion (1.6)	0.3697	0.2606	0.6243
Random diffusion (1.5)	0.4901	0.2704	-2.9092

The infection fraction and the two segregation indices of the four models are given in Table 4. In this example, the two models with symmetric and homogeneous diffusions have positive segregation indices $\chi(S, I)$, which means that these two cases are segregated poorly. However, the sizes of the infected population of these two cases are smaller than other two cases. On the other hand, the other two cases with random diffusion and ODE models have negative segregation indices χ. This implies that the segregation indices mean little in this example.

6. Concluding remarks

In this paper, we considered two SIS reaction-diffusion epidemic models, (1.6) with a symmetric diffusion of Fickian diffusion type and (1.5) with a random diffusion of Fokker-Planck diffusion type [19, 24]. We assumed that the diffusion rate $f(x)$ of the susceptible population is proportional to the transmission rate $\beta(x)$ and the diffusion rate $g(x)$ of the infected population is reversely proportional to the recovery rate $r(x)$. The paper consists of a mathematical analysis part and a numerical computation part.

Analytically, we have shown the well-posedness of (1.5) and (1.6) (Propositions 2.1–3.1), obtained the basic reproduction number $\mathcal{R}_0$ using a variational method, and shown the monotonicity and the asymptotic behavior of $\mathcal{R}_0$ in terms of g (Lemmas 2.2–3.3). Next, we have shown the existence, uniqueness, and stability of the DFE of (1.6) (Theorem 2.2). Since the diffusion of (1.6) is not homogeneous, we could not apply the methods in [1] to study the existence and uniqueness of the EE of (1.6). Fortunately, we can utilize the persistence theory in [34] to show that system (1.6) is persistent when $\mathcal{R}_0 > 1$, thus ensuring that there exists at least one EE (Theorem 2.3). In addition, we have shown the existence, uniqueness, and stability of DFE and EE for the model (1.5) (Theorems 3.2-3.3). Note that we generalized the relevant results in [1, Lemmas 2.2-2.3] (see Lemmas 2.1, 2.2, 3.2, and 3.3).

In section 4, we numerically tested the analytical results in sections 2 and 3. In order to see the role of the spatial heterogeneity and the diffusion models on the disease transmission, we tested the effects of the infection rate $\beta(x)$ and the diffusion rate $g(r^{-1}(x))$ on $\mathcal{R}_0$ for models (1.5) and (1.6) (Figs. 2 and 5). Moreover, we drew the sample solutions for systems (1.5) and (1.6) when $\mathcal{R}_0 > 1$ and $\mathcal{R}_0 < 1$ respectively (Figs. 3, 4, 6, and 7). Note that we have obtained the existence of endemic equilibrium for models (1.5) and (1.6), but the stability of EE is open for future study.

In section 5, three examples are numerically tested to see the effect of heterogeneous diffusion in the disease spread. It is widely believed that diffusion homogenizes substances. However, in the first example, we observed that a heterogeneous random diffusion segregates infected and susceptible populations further than an ODE model and thus reduces the size of the infected population (see Fig. 8 and Table 1). However, symmetric diffusion never does that. In the second example, the random diffusion decreases segregation indices but still reduces the size of the infected population by moving infected individuals to a disease-free region (see Fig. 9 and Table 2; Fig. 10 and Table 3). Usually, the heterogeneous random diffusion model takes a smaller infected population size since $f(x) = \beta(x)$ and $g(x) = r^{-1}(x)$. However, depending on the situation, such a strategy may increase the infected population size. The third example is such a case (see Fig. 11 and Table 4). We should remember the various effects of heterogeneous random diffusion on the disease transmission. The numerical tests in section 5 show some interesting effects, which can help us further understand the transmission mechanism of diseases and provide effective strategies for disease control.

It should be pointed out that in Theorem 2.3, we only obtain the existence of the endemic equilibrium, not the uniqueness. The uniqueness is therefore left for future investigation. On the other hand, as we all know, many infectious diseases have incubation periods, and populations can move randomly during the period. This means that the infection thereby depends not only on the interaction at the current location and time, but also on the interaction of all possible locations at previous times [29]. The susceptibility of a susceptible highly depends on the distance from each adjacent infectious individual. Such a infection mechanism is often modeled by a nonlocal incidence with a kernel function whose support determines the effective infection area [16]. Therefore, it seems necessary to incorporate nonlocal effects and/or delay into epidemic modeling. Future endeavor should explore the influences of nonlocality or delay on the segregation phenomenon.

Acknowledgements

We would like to thank Fengqi Yi for the initial discussion. H. Wang was partially supported by Natural Sciences and Engineering Research Council of Canada (Individual Discovery Grant RGPIN-2020-03911 and Discovery Accelerator Supplement Award RGPAS-2020-00090). K. Wang was partially supported by Postgraduate Research & Practice Innovation Program of Jiangsu Province (No. KYCX20_0169) and Nanjing University of Aeronautics and Astronautics PhD short-term visiting scholar project (ZDGB2021026) at the University of Alberta. Y.-J. Kim was partially supported by National Research Foundation of Korea (NRF-2017R1A2B2010398).

References

1. L. J. S. Allen, B. M. Bolker, Y. Lou, and A. L. Nevai, *Asymptotic profiles of the steady states for an SIS epidemic reaction-diffusion model*, Discrete Contin. Dyn. Syst., **21** (2008) 1-20.
2. E. Cho, Y.-J. Kim, *Starvation driven diffusion as a survival strategy of biological organisms*, Bull. Math. Biol., **75** (2013) 845-870.

3. R. Cui, Y. Lou, *A spatial SIS model in advective heterogeneous environments*, J. Differ. Equ., **261** (2016) 3305-3343.
4. R. Cui, K.-Y. Lam, Y. Lou, *Dynamics and asymptotic profiles of steady states to an epidemic model in advective environments*, J. Differ. Equ., **263** (2017) 2343-2373.
5. K. Deng, Y. Wu, *Global attractivity of delayed and nonlocal diffusive logistic models with variable coefficients*, J. Differ. Equ., **299** (2021) 229-255.
6. L. Dung, *Dissipativity and global attractors for a class of quasilinear parabolic systems*, Commun. Partial Differ. Equ., **22** (3–4) (1997) 413-433.
7. J. Ge, K.I. Kim, Z.-G. Lin, H.-P. Zhu, *A SIS reaction-diffusion-advection model in a low-risk and high-risk domain*, J. Differ. Equ., **259** (2015) 5486-5509.
8. J.K. Hale, *Asymptotic Behavior of Dissipative Systems*, American Mathematical Society, Providence, 1988.
9. D. Henry, *Geometric Theory of Semilinear Parabolic Equations*, Springer-Verlag, New York, 1981.
10. Y.-J. Kim, O. Kwon, Fang Li, *Evolution of dispersal toward fitness*, Bull. Math. Biol., **75** (2013) 2474-2498.
11. Y.-J. Kim, O. Kwon, Fang Li, *Global asymptotic stability and the ideal free distribution in a starvation driven diffusion*, J. Math. Biol., **68** (2014) 1341-1370.
12. Y.-J. Kim, H. Seo, C. Yoon, *Asymmetric dispersal and evolutional selection in two-patch system*, Discret. Contin. Dyn. Syst., **40** (2019) 3571-3593.
13. M.G. Krein, M.A. Rutman, *Linear operators leaving invariant a cone in a Banach space*, Am. Math. Soc. Transl., **10** (1) (1962) 3-95.
14. K. Kuto, H. Matsuzawa, R. Peng, *Concentration profile of endemic equilibrium of a reaction-diffusion-advection SIS epidemic model*, Calc. Var. Partial Differential Equations., **56** (2017) 112.
15. H.-C. Li, R. Peng, F.-B. Wang, *Varying total population enhances disease persistence: qualitative analysis on a diffusive SIS epidemic model*, J. Differ. Equ., **262** (2017) 885-913.
16. Z. Liu, Z. Shen, H. Wang, Z. Jin, *Analysis of a local diffusive SIR model with seasonality and nonlocal incidence of infection*, SIAM J. on Appl. Math., 79 (2019) 2218-2241.
17. Y. Lou, T. Nagylaki, *Evolution of a semilinear parabolic system for migration and selection without dominance*, J. Diff. Eqns., **225** (2006) 624-665.
18. P. Magal, X.-Q. Zhao, *Global attractors and steady states for uniformly persistent dynamical systems*, SIAM J. Appl. Math., **37** (2005) 251-275.
19. A. Okubo, S. Levin, *Diffusion and Ecological Problems*, Springer, NY, 2001.
20. C.V. Pao, *Nonlinear Parabolic and Elliptic Equations*, Plenum, New York, 1992.
21. R. Peng, *Asymptotic profiles of the positive steady state for an SIS epidemic reaction–diffusion model. Part I*, J. Differ. Equ., **247** (2009) 1096-1119.
22. R. Peng, S. Liu, *Global stability of the steady states of an SIS epidemic reaction–diffusion model*, Nonlinear Anal. TMA., **71** (2009) 239-247.
23. R. Peng, X.Q. Zhao, *A reaction-diffusion SIS epidemic model in a time-periodic environment*, Nonlinearity, **25** (2012) 1451-1471.
24. A. Potapov, U. Schlägel, M.A. Lewis, *Evolutionarily stable diffusive dispersal*, Discret. Contin. Dyn. Syst. B., 19 (2014) 3319-3340.
25. M.H. Protter, H.F. Weinberger, *Maximum Principles in Differential Equations*, 2nd ed., Springer-Verlag, Berlin, 1984.
26. T. Schelling, *Models of segregation*, American Economic Review, Papers and Proceedings, **59** (1969) 488-493.
27. J. Smoller, *Shock waves and reaction-diffusion equations*, Springer Verlag, New York, 1983.
28. H. Wang, Y. Salmaniw, *PDE guidance for cognitive animal movement*, https://arxiv.org/abs/2201.09150, under review.
29. K. Wang, H. Zhao, H. Wang, R. Zhang, *Traveling wave of a reaction–diffusion vector-borne disease model with nonlocal effects and distributed delay*, J. Dyn. Differ. Equ., (2021) https://doi.org/10.1007/s10884-021-10062-w.
30. W. Wang, X.-Q. Zhao, *Basic reproduction numbers for reaction-diffusion epidemic models*, SIAM J. Appl. Dyn. Syst., 11 (2012) 1652-1673.
31. X. Wang, H. Wang, M. Li, *Modeling rabies transmission in spatially heterogeneous environments via θ-diffusion*, Bull. Math. Biol., **83** (2021) 1-38.
32. Y. Wu, X. Zou, *Asymptotic profiles of steady states for a diffusive SIS epidemic model with mass action infection mechanism*, J. Differ. Equ., **261** (2016) 4424-4447.
33. H. Zhao, K. Wang, H. Wang, *Basic reproduction ratio of a mosquito-borne disease in heterogeneous environment*, under review.
34. X.-Q. Zhao, *Dynamical Systems in Population Biology*, 2nd edn. Springer, New York, 2017.